Preprints.org

Review

Not peer-reviewed version

High-Frequency and Ultra-High-Frequency Ultrasound in Dermatologic Diseases and Aesthetic Medicine

Giulio Argalia , Alfonso Reginelli , Elisa Molinelli , Anna Russo , Alessandra Michelucci , Andrea Sechi , Angelo Valerio Marzano , Stella Desyatnikova , Marco Fogante , Vittorio Patanè , Giammarco Granieri , Corrado Tagliati * , Giulio Rizzetto , Edoardo De Simoni , Marco Matteucci , Matteo Candelora , Cecilia Lanza , Claudio Ventura , Nicola Carboni , Roberto Esposito , Stefano Esposito , Massimiliano Paolinelli , Elisabetta Esposto , Giuseppe Lanni , Gabriella Lucidi Pressanti , Chiara Giorgi , Fabiola Principi , Alberto Rebonato , Sylwia Patrycja Malinowska , Robert Krzysztof Mlosek , Gian Marco Giuseppetti , Valentina Dini , Marco Romanelli , Annamaria Offidani , Salvatore Cappabianca , Ximena Wortsman , Oriana Simonetti

Posted Date: 24 December 2024

doi: 10.20944/preprints202412.1938.v1

Keywords: dermatology; high-frequency ultrasound; ultra-high-frequency ultrasound

Preprints.org is a free multidisciplinary platform providing preprint service that is dedicated to making early versions of research outputs permanently available and citable. Preprints posted at Preprints.org appear in Web of Science, Crossref, Google Scholar, Scilit, Europe PMC.

Copyright: This open access article is published under a Creative Commons CC BY 4.0 license, which permit the free download, distribution, and reuse, provided that the author and preprint are cited in any reuse.

Preprints.org (www.preprints.org) | NOT PEER-REVIEWED | Posted: 24 December 2024 doi:10.20944/preprints202412.1938.v1

Disclaimer/Publisher's Note: The statements, opinions, and data contained in all publications are solely those of the individual author(s) and contributor(s) and not of MDPI and/or the editor(s). MDPI and/or the editor(s) disclaim responsibility for any injury to people or property resulting from any ideas, methods, instructions, or products referred to in the content.

Review

High-Frequency and Ultra-High-Frequency Ultrasound in Dermatologic Diseases and Aesthetic Medicine

Giulio Argalia [1], Alfonso Reginelli [2], Elisa Molinelli [3], Anna Russo [2], Alessandra Michelucci [4,5], Andrea Sechi [6], Angelo Valerio Marzano [6,7], Stella Desyatnikova [8], Marco Fogante [1], Vittorio Patanè [2], Giammarco Granieri [4], Corrado Tagliati [9,*], Giulio Rizzetto [3], Edoardo De Simoni [3], Marco Matteucci [3], Matteo Candelora [3], Cecilia Lanza [1], Claudio Ventura [1], Nicola Carboni [1], Roberto Esposito [10], Stefano Esposito [11], Massimiliano Paolinelli [12], Elisabetta Esposto [13], Giuseppe Lanni [14], Gabriella Lucidi Pressanti [14], Chiara Giorgi [15], Fabiola Principi [16], Alberto Rebonato [17], Sylwia Patrycja Malinowska [18], Robert Krzysztof Mlosek [19], Gian Marco Giuseppetti [20], Valentina Dini [4], Marco Romanelli [4], Annamaria Offidani [3], Salvatore Cappabianca [2], Ximena Wortsman [21,22,23,24] and Oriana Simonetti [3]

[1] Maternal-Child, Senological, Cardiological Radiology and Outpatient Ultrasound, Department of Radiological Sciences, University Hospital of Marche, via Conca 71, 60126 Ancona, Italy
[2] Department of Precision Medicine, University of Campania Luigi Vanvitelli, piazza Luigi Miraglia 2, 80131 Naples, Italy
[3] Department of Clinical and Molecular Sciences, Dermatology Clinic, Polytechnic Marche University, via Conca 71, 60126 Ancona, Italy
[4] Department of Dermatology, University of Pisa, via Roma 67, 56126 Pisa, Italy
[5] Interdisciplinary Center of Health Science, Sant'Anna School of Advanced Studies of Pisa, piazza Martiri della Libertà 33, 56127 Pisa, Italy
[6] Dermatology Unit, Fondazione IRCCS Ca' Granda Ospedale Maggiore Policlinico, via Pace 9, 20122 Milan, Italy
[7] Department of Pathophysiology and Transplantation, Università degli Studi di Milano, via Francesco Sforza 35, 20122 Milan, Italy
[8] The Stella Center for Facial Plastic Surgery, 509 Olive Way Ste 1430, Seattle, WA 98101, USA
[9] AST Ancona, Ospedale di Comunità Maria Montessori di Chiaravalle, via Fratelli Rosselli 176, Chiaravalle, 60033 Ancona, Italy
[10] Gemini Med Diagnostic Clinic, via Tabellione 1, 47891 Falciano, Repubblica di San Marino
[11] Poliambulatorio CPV, via Vivaldi 2-4, Loreto, 60025 Ancona, Italy
[12] AST Ancona, Distretto sanitario di Senigallia, Dermatologia, via Campo Boario 4, Senigallia, 60019 Ancona, Italy
[13] AST Pesaro-Urbino; Distretto sanitario di Pesaro, via XI Febbraio, 61121 Pesaro, Italy
[14] Department of Services, U.O.S.D. Radiology, San Liberatore Hospital, viale Risorgimento, Atri, 64032 Teramo, Italy
[15] AST Pesaro-Urbino, Radiologia, Ospedale Santa Maria della Misericordia, via Comandino 70, 61029 Urbino, Italy
[16] AST Ancona, Radiologia, Ospedale Santa Casa di Loreto, via San Francesco 1, Loreto, 60025 Ancona, Italy
[17] AST Pesaro-Urbino, Radiologia, Ospedale San Salvatore, piazzale Cinnelli 1, 61121 Pesaro, Italy
[18] Life-Beauty—Private Company, Ul. T. Kosciuszki 29, 05-825 Grodzisk Mazowiecki, Poland
[19] Diagnostic Ultrasound Laboratory, Medical University of Warsaw, 61 Zwirki i Wigury Street, 02-091 Warszawa, Poland
[20] Medical Point Ancona, via Trieste 21, 60124 Ancona, Italy
[21] Department of Dermatology, Faculty of Medicine, Universidad de Chile, Lo Fontecilla 201 of 734 Las Condes, Región Metropolitana de Santiago 8330111, Chile
[22] Department of Dermatology, School of Medicine, Pontificia Universidad Catolica de Chile, Av. Libertador Bernardo O'Higgins 340, Región Metropolitana de Santiago 8331150, Chile
[23] Institute for Diagnostic, Imaging and Research of the Skin and Soft Tissues (IDIEP), Lo Fontecilla 201 of 734 Las Condes, Región Metropolitana de Santiago 7591018, Chile
[24] Department of Dermatology and Cutaneous Surgery, Miller School of Medicine, University of Miami, 1120 NW 14th St Ste 9, Miami, FL 33146, USA
* Correspondence: corradotagliati@gmail.com; Tel.: +393662677166

Abstract: Dermatologic ultrasonography applications are rapidly growing in all skin fields. Thanks to very high spatial resolution, high-frequency and ultra-high-frequency ultrasound can evaluate smaller structures allowing us to improve diagnosis accuracy and disease activity. Moreover, they can guide treatment, such as drug injection, and assess therapy efficacy and complications. In this narrative review, we evaluated high-frequency ultrasound and ultra-high-frequency ultrasound in

© 2024 by the author(s). Distributed under a Creative Commons CC BY license.

Preprints.org (www.preprints.org) | NOT PEER-REVIEWED | Posted: 24 December 2024 doi:10.20944/preprints202412.1938.v1

infections, inflammatory dermatoses, metabolic and genetic disorders, specific cutaneous structure skin disorders, vascular and external agents associated disorders, neoplastic diseases, and aesthetics

Keywords: dermatology; high-frequency ultrasound; ultra-high-frequency ultrasound

1. Introduction

Many imaging modalities have been used in dermatology, some for a long time, such as dermoscopy, and others newer, such as optical coherence tomography and reflectance confocal microscopy [1].

Radiologists can evaluate skin and skin-related disorders through ultrasound, X-ray, computed tomography, magnetic resonance imaging, and positron emission tomography.

The imaging modality that both radiologists and dermatologists perform is ultrasound. New advancements such as high and ultra-high frequency ultrasound allow us to evaluate better skin layers and diseases.

Linear probes with frequencies of 15 MHz or greater are needed to evaluate skin layers [2]. High-frequency ultrasound (HFUS) is usually considered when a 20-30 MHz transducer is used, allowing tissue penetration of about 10 mm, which is useful for dermis and subcutaneous tissue evaluation. Ultra-high-frequency ultrasound (UHFUS) is defined when probes with higher frequencies are used, with a penetration depth of about 3 and 4 mm, respectively, for 48 MHz and 70 MHz probes, which allow a better evaluation of epidermis, hair follicles, nail units, and vessels, including lymphatics [3-6] (Figure 1).

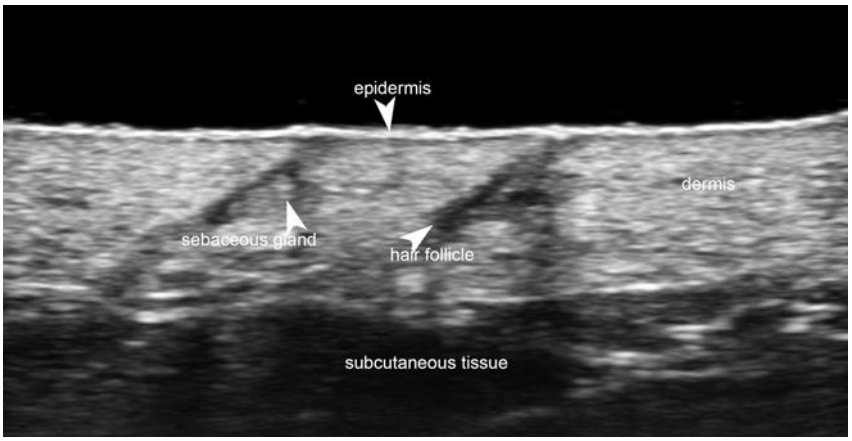

Figure 1. Normal non-glabrous skin at 70 MHz with a superficial bright hyperechoic monolaminar layer, which is the epidermis, a thicker but less hyperechoic band that corresponds to the dermis, and a deeper hypoechoic structure that represents the subcutaneous tissue. Notice the hyperechoic oval-shaped structure of the sebaceous gland and a hypoechoic oblique band, that corresponds to the hair follicle. .

In this narrative review, we evaluated HFUS and UHFUS in infections, inflammatory dermatoses, metabolic and genetic disorders, specific cutaneous structure skin disorders, vascular and external agents-associated disorders, neoplastic diseases, and aesthetics.

2. Infections

Ultrasound is useful in an emergency department setting to differentiate between abscesses and other skin and soft tissue infections such as cellulitis; this is very important, as abscesses can be managed using drainage, whereas cellulitis can be treated with antibiotics [7]. This differentiation can also be reached in the pediatric population, in which a rapid, non-invasive, painless, easily repeatable ultrasound examination can allow for a change in the management of an equivocal

Preprints.org (www.preprints.org) | NOT PEER-REVIEWED | Posted: 24 December 2024 doi:10.20944/preprints202412.1938.v1

physical examination [8]. Abscesses are irregular, hypoechoic, or anechoic lesions with variable echogenic debris, surrounded by a hyperechoic rim and peripheral hypervascularity; cellulitis can show diffuse dermis and subcutis thickening with hyperechoic "cobblestone" appearance, and increased vascularity (Figures 2-4) [9].

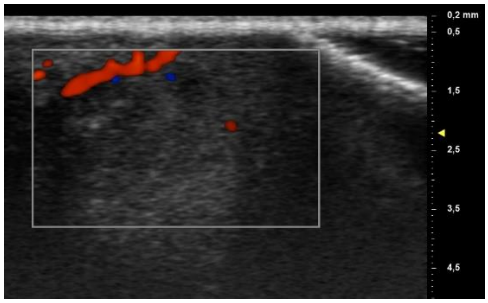

Figure 2. Third toe abscess at color-Doppler 70 MHz image.

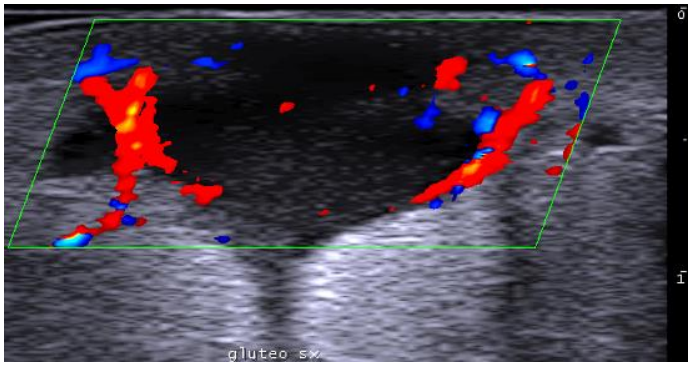

Figure 3. Abscess at color-Doppler 20 MHz image.

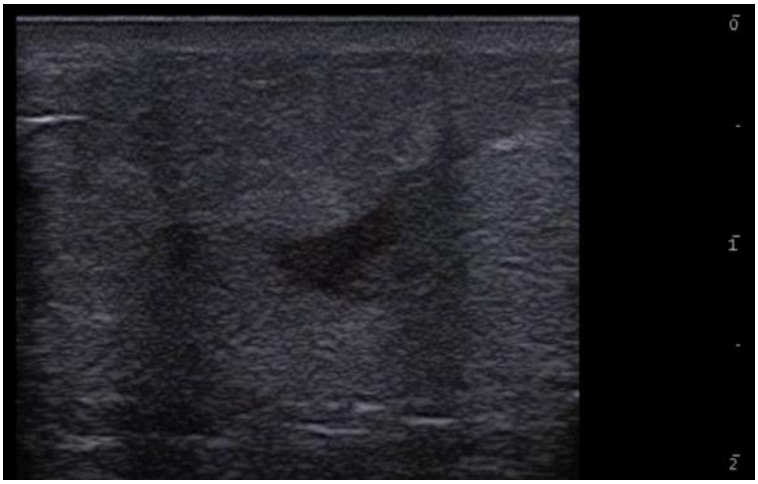

Figure 4. Grayscale 20MHz ultrasound image of erysipelas shows a thickened, hyperechoic dermis with a hypoechoic band of fluid and hyperechoic surrounding subcutaneous edema, without abscess formation.

In cases in which clinical examination or dermoscopy are non-conclusive for scabies, HFUS can help identify the mites as hyperechoic, millimetric structures within the epidermis or at the epidermal-dermal junction, and their burrows as linear or curvilinear hypoechoic tracks in the stratum corneum; moreover, HFUS can help assessing treatment accuracy and efficacy, as real mites

Preprints.org (www.preprints.org) | NOT PEER-REVIEWED | Posted: 24 December 2024 doi:10.20944/preprints202412.1938.v1

presence or absence within the epidermis of non-specific burrow-like scratches can be evaluate in patients with persistent pruritus [10].

Warts are caused by the human papillomavirus and appear on ultrasound as focal fusiform hypoechoic epidermal and dermal structures, with irregular epidermis and dermal thickening, and commonly hypervascularity on Doppler examination; ultrasound can help monitor treatment responses, particularly in recurrent and difficult cases with persistent pain [11].

HFUS allows the evaluation of odontogenic cutaneous sinus tract, and plays a crucial diagnostic role, as frequently it is not clinically suspected; in fact, a nodular, triangular, or mushroom-shaped lesion can be detected in the subcutis, which continues with a slightly tortuous band structure, up to the focally interrupted cortical bone plate; hypervascularity around and/or within the lesion due to inflammation, and a hard strain elastography pattern of the sinus tract due to fibrous and granulomatous tissue are reported [12].

Moreover, HFUS can be used in other skin infections to evaluate better epidermis, dermis, and subcutis and their alterations, such as epidermal thickening, dermal disorganization, dermal decreased echogenicity, subcutis hyperechogenicity, and increased vascularization in chromoblastomycosis [13].

HFUS is reported to be very useful in the diagnosis, evaluation of deep hypodermal involvement, intralesional ultrasound-guided drug infiltration and follow-up of cutaneous leishmaniasis [14-16]; moreover, ultrasound can help differentiate two disease patterns, inflammatory and pauci-inflammatory ones, with lower healing time for lesions with pauci-inflammatory pattern (Figure 5); in fact, inflammatory pattern showed central vascularity, ill-defined margins, and more signs of panniculitis than pauci-inflammatory one [16] (Figure 6).

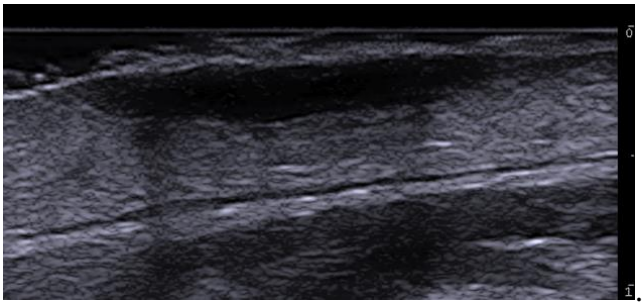

Figure 5. Greyscale 20MHz ultrasound image of cutaneous leishmaniasis showing well-defined, homogenous hypoechoic dermal structure (between markers), with minimal reactive changes in the underlying hypodermis (pauci-inflammatory pattern).

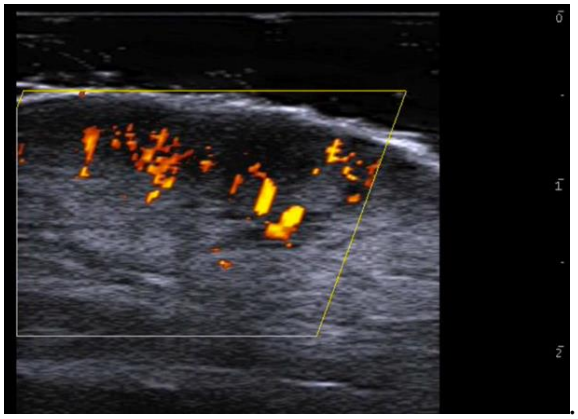

Figure 6. Power Doppler 20MHz ultrasound image of an ulcerated plaque of cutaneous leishmaniasis shows a diffuse central vascular signal (inflammatory pattern).

Preprints.org (www.preprints.org) | NOT PEER-REVIEWED | Posted: 24 December 2024 doi:10.20944/preprints202412.1938.v1

HFUS is reported to be the best imaging technique for the evaluation of nerve disease in leprosy, particularly for the assessment of ulnar, median, common fibular and tibial neuropathy in Hansen's disease without evident skin involvement, as leprosy primarily involves Schwann cells and secondarily affects the skin and mucous membrane with anaesthetic patches or deformities; when a pure neuritic Hansen's disease is detected assessing peripheral nerve cross-sectional area immediate treatment is necessary to prevent complication, as if the skin is already involved, it is usually too late to prevent them; moreover, asymmetric multiple nerve thickening or asymmetry could indicate evidence of Hansen's disease neuropathy among household contacts of patients with leprosy, and this could become a useful tool for an early diagnosis of leprosy cases [17-19].

HFUS and UHFUS can help diagnose, and monitor the treatment and better understand the spreading mechanisms of cutaneous larva migrans, as the larva can be identified as a small linear hyperechoic subepidermal structure, the dilated lymphatic ducts can be detected as hypoechoic dermal and hypodermal tunnels, inflammation can be revealed by hypoechoic dermis, hyperechoic subcutis and increased vascularity on color-Doppler imaging [20]. Fly larvae (myasis) can cause skin infestation, and on HFUS central hyperechoic moving structure can be shown, with hypoechoic rim and peripheral vascularity on color Doppler [21].

Actinomycetomas and eumycetomas can show hypoechoic areas or connecting tracts with increased rim vascularity [22].

In patients with gonorrhea, ultrasound can demonstrate paraurethral ducts diameter and length before and after treatment and can guide incision, drainage, and wedge resection when antibiotics are not sufficient [23, 24].

3. Inflammatory Dermatoses

Plaque psoriasis shows increased thickness of the epidermis and dermis, with frequent epidermal thickening and undulation with dermal hypoechogenicity due to inflammation, and lack of subcutis abnormalities [25, 26]

Lichen planus papules can demonstrate increased thickness and a decreased echogenicity of the upper dermis, with hypoechoic dermis, related to epidermal acanthosis and dermal inflammatory infiltrate [27, 28].

The upper dermal hypoechoic band thickness significantly decreases during dupilumab treatment, and it shows a high correlation with clinical scores in patients with moderate or severe atopic dermatitis [29-32] (Figures 7 and 8).

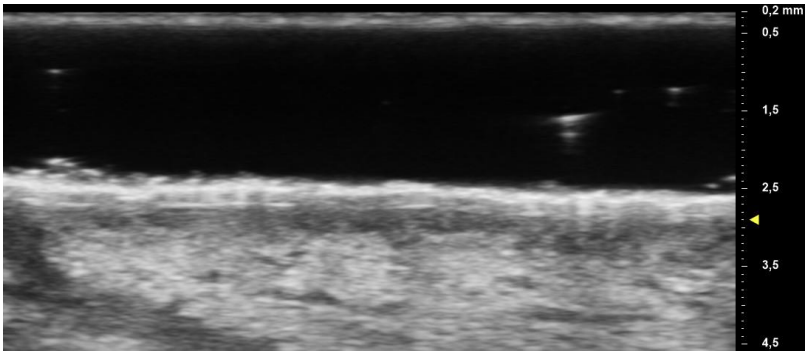

Figure 7. B-Mode 70MHz ultrasound image of atopic dermatitis with evident decreased echogenicity of the upper dermis.

Preprints.org (www.preprints.org) | NOT PEER-REVIEWED | Posted: 24 December 2024 doi:10.20944/preprints202412.1938.v1

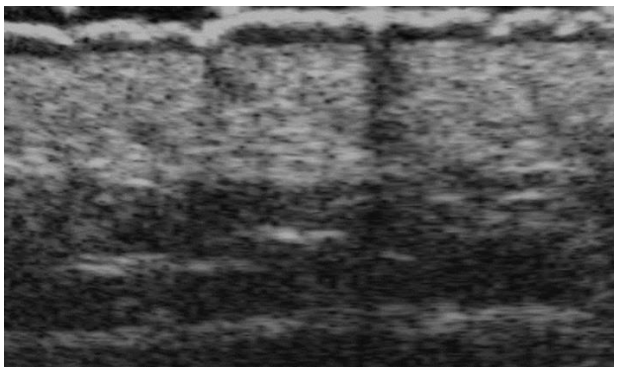

Figure 8. Atopic dermatitis with evident hypoechoic upper dermal band at 48 MHz.

Epidermial irregularity and hyperechogenicity, hypoechoic linear band at the dermo-epidermal junction, and modest dermal thickening were found in seborrheic dermatitis [33].

In cutaneous chronic graft-versus-host disease, HFUS can show an epidermis and subcutis thinning and a dermis thickening compared to healthy controls; moreover, HFUS could help obtain an earlier diagnosis of this disease [34].

A widened and hypoechoic dermis, hypoechoic dermal areas, hypo-anechoic fusiform structures below the epidermis representing localized infiltrate, cutaneous and subcutaneous edema with superficial thrombophlebitis and chronic thrombosis with punctate intraluminal calcifications are possible imaging findings in cutaneous mastocytosis [35, 36].

UHFUS in pyoderma gangrenosum can show hyperechoic oval structures and hair tract in the inflammatory phase, and the identification of these early inflammatory imaging signs could, in the future, let dermatologists avoid biopsies to diagnose this disease [37] (Figure 9).

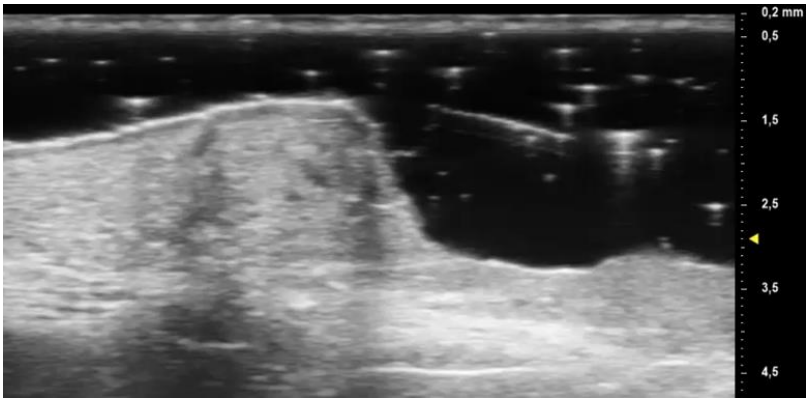

Figure 9. B-Mode 70MHz ultrasound image of a pyoderma gangrenosum lesion.

UHFUS can accurately assess epidermal, dermal, and subcutis thickness, and precisely identify the epidermal-dermal junction and the boundary between the dermis and subcutaneous tissue [38]. Therefore, it could be useful to differentiate blister locations, such as subepidermal and intraepidermal bullae, respectively, in bullous pemphigoid and pemphigus vulgaris [39] (Figures 10 and 11). Moreover, intraoral UHFUS can help differentiate between oral pemphigus vulgaris and mucous membrane pemphigoid, as statistically significant differences between the echogenicity of these two lesions were identified [40].

Preprints.org (www.preprints.org) | NOT PEER-REVIEWED | Posted: 24 December 2024 doi:10.20944/preprints202412.1938.v1

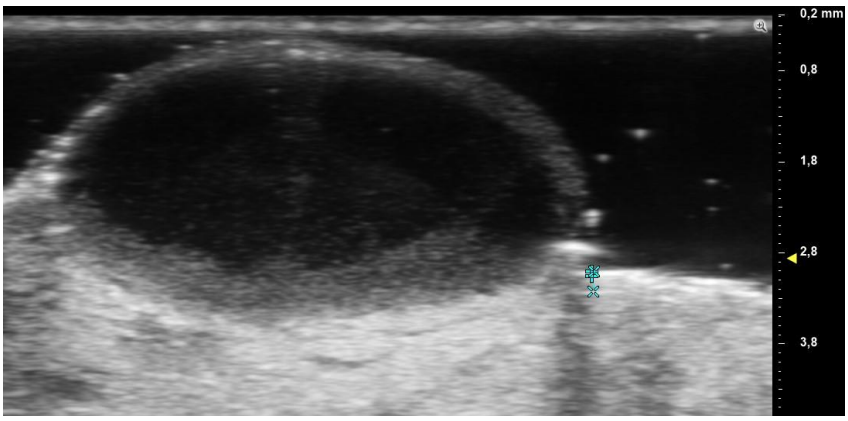

Figure 10. Subepidermal blister in bullous pemphigoid at 70MHz.

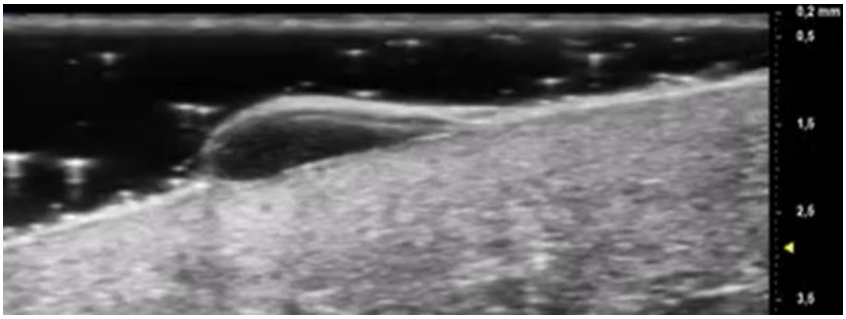

Figure 11. Intraepidermal blister in pemphigus vulgaris at 70MHz.

Ultrasound can present vascular density reduction in the fingertip with a higher resistive index due to vascular wall damage in lupus erythematosus patients, and UHFUS can show hypoechoic zone at dermo-epidermal junction and superficial dermis in neonatal lupus erythematosus annular erythema due to inflammatory cells infiltration [41, 42].

Lupus panniculitis can be detected as a subcutis mild hyperechoic ovoidal pseudo-mass with hypoechoic margin and increased vascularization on color-Doppler imaging [43]. Connective tissue panniculitis is a rare cutaneous manifestation of connective tissue diseases associated with lupus erythematosus and dermatomyositis, and HFUS can help reach an early diagnosis in cases with unclear skin symptoms; moreover, HFUS can allow a non-invasive clinical decision making, as active connective tissue panniculitis is correlated to the hypoechoic dermis, undefined epidermal-dermal borders, hypodermal thickening and hypoechoic septa, hyperechoic lobules, the presence of vessel diameter of more than 1 mm, systolic peak > 10 cm/s and resistance index > 0.7 MHz at color Doppler imaging [44].

Ultrasonography can allow us to discriminate mostly lobular from mostly septal panniculitis. This is relevant since lobular and septal panniculitis are usually due to different entities [45] (Figure 12).

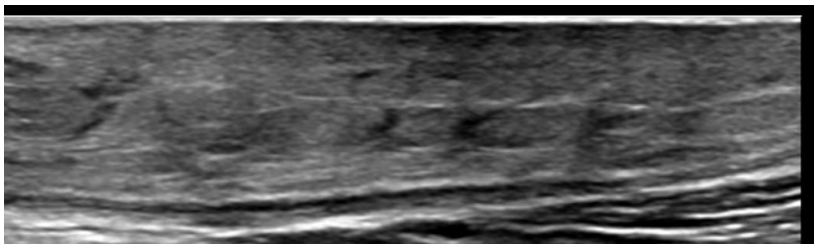

Figure 12. Panniculitis with hyperechoic lobules and hypoechoic septa in a thickened hypodermis using a 20 MHz probe.

Preprints.org (www.preprints.org) | NOT PEER-REVIEWED | Posted: 24 December 2024 doi:10.20944/preprints202412.1938.v1

In systemic lupus erythematosus patients, a higher intima media thickness was found in various arterial territories than in healthy controls, with a medium echogenic appearance due to possible inflammation or early atherosclerosis [46]. Moreover, HFUS showed a thicker carotid intima and a thinner carotid media in premenopausal women with systemic lupus erythematosus compared to age-matched healthy controls [47]. US can also detect early articular and periarticular disease, such as joint effusion and synovitis, and in rhupus syndrome cortical erosions can be detected [48].

Ultrasound can be helpful to diagnose rheumatoid nodules in finger tendons as a screening procedure in rheumatoid arthritis patients [49].

UHFUS presented epidermal hypoechogenicity and thickening, as well as dermal hypoechogenicity in systemic sclerosis patients, compared to healthy controls [50]. HFUS of the skin between the nail fold and the distal interphalangeal joint can show skin thickening that is higher than in healthy controls or patients with primary Raynaud's phenomenon [51]. Moreover, UHFUS can help assess digital arteries vasculopathy as all three finger arterial layers were significantly thicker in systemic sclerosis patients than in healthy controls [52].

Inflammatory phase morphea shows dermal thickening and hypoechogenicity with subcutaneous increased vascularity and echogenicity, causing dermal-hypodermal blurredness. At the sclerotic phase, there is dermal thinning and dermal hyperechogenicity, subcutaneous thinning and hyperechogenicity; moreover, color-Doppler ultrasound can frequently detect subclinical activity in areas adjacent to the clinically active lesion, in nonadjacent regions, and at a clinically inactive lesion site; in fact, ultrasound morphea activity scoring can better support a systematical description of the cutaneous abnormalities and activity tracking accuracy, and evaluate treatment response [53-61]; ultrasound allows morphea early diagnosis which is essential to avoid serious consequences of atrophy and fibrosis, also after a trigger such as liposuction [62].

Cutaneous sarcoidosis burden can be objectively evaluated using UHFUS and this new non-invasive disease severity measure correlates with histopathology and clinical evaluation potentially obviating subjective clinical assessment and biopsies necessity [63, 64].

4. Metabolic and Genetic Disorders

Primary localized cutaneous nodular amyloidosis can show subcutis hypoechoic lesion with linear calcifications, and it should be considered among the diseases that can show dystrophic calcifications, such as autoimmune connective tissue diseases, scleroderma, and cutaneous lupus erythematosus [65].

Scleredema diabeticorum can present evident dermal thickening with hyperechoic foci and reduced visualization of the deep dermis [66].

Ultrasonography can be applied to evaluate better, follow-up and detect early changes in localized pretibial myxoedema in Graves's disease, in which a hypoechoic thickened dermis and subcutis with ill-defined dermis-hypodermis boundaries can be observed [67].

Ultrasound can allow us to diagnose or confirm the presence of clinically suspected calcinosis cutis (Figure 13), to guide intralesional drug injection such as sodium thiosulfate, and to evaluate treatment response [68, 69].

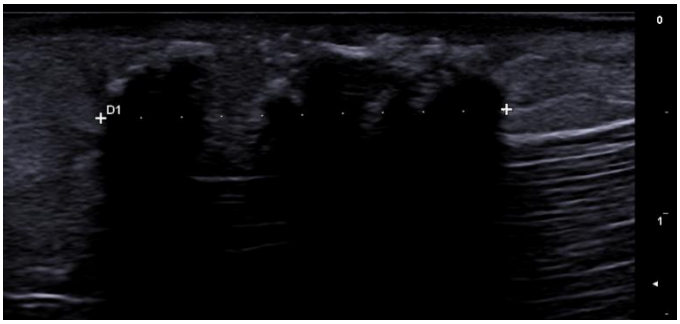

Preprints.org (www.preprints.org) | NOT PEER-REVIEWED | Posted: 24 December 2024 doi:10.20944/preprints202412.1938.v1

Figure 13. Right elbow subcutaneous calcifications in a patient with systemic sclerosis using a 24 MHz probe.

Ultrasound can be used to evaluate diabetic foot ulcers healing quantitatively, and UHFUS of the big toe showed upper dermal hypoechogenicity and thickening, probably due to papillary dermal edema; moreover, epidermis was reported to be thinner in patients with diabetic neuropathy and previous ulcers [70-72].

In patients with X-linked dominant protoporphyria HFUS of the nasal dorsum showed epidermal thickening and dermal hypoechogenicity [73].

Plantar foot calluses in patients with pachyonychia congenita showed an anechoic structure between the epidermis and dermis, due to subepidermal blister fluid; this characteristic was not reported in patients with other forms of palmoplantar keratoderma, such as mal de Meleda and epidermolytic palmoplantar keratoderma [74].

Pseudoxanthoma elasticum skin lesions are oval homogeneous hypoechogenic areas in the mid and deep dermis related to the presence of glycosaminoglycans and a high level of hydration of connective tissue; moreover, undulating skin surface with normal epidermis and dermal/epidermal interface are reported, without significantly skin echogenic structure due to the small size of the dermal elastic fiber calcifications [75] (Figure 14).

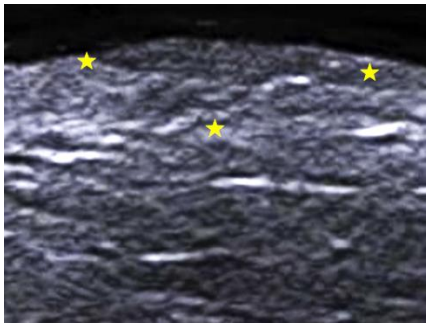

Figure 14. Greyscale 20 MHz ultrasound of pseudoxanthoma elasticum on the neck. The involved area is limited by yellow stars and shows a mild decrease in dermal echogenicity in a small single papular lesion.

5. Specific Cutaneous Structure and Sites of Skin Disorders

HFUS can evaluate different forms and phases of primary cicatricial alopecia; in fact, inactive phase showed a lower number or a lack of follicular structures compared to active phase; active discoid lupus erythematosus showed widened follicular structures with hypoechogenic bands; lichen planopilaris and frontal fibrosing alopecia showed cigar-like shaped follicular structures in active phase, whereas during inactive phase exhibited irregular and saw-like dermal-subepidermal boundary [76].

UHFUS can evaluate and differentiate between active, inactive and regrowth phases of alopecia areata; therefore, HFUS can be very useful for disease prognosis [77, 78]. The three most common ultrasound features are empty hair follicles, small ovoid hair follicles and subcutis perifollicular hyperechogenicity [79].

Small ovoid hair follicles and miniaturized hairs were also detectable in female pattern hair loss and senescent alopecia. Active lichen planopilaris and frontal fibrosing alopecia lesions showed perifollicular hypoechogenicity in the mid-dermis and distal ambiguity of hair follicles. Homogeneous dermis without structures was detected in lichen planopilaris and frontal fibrosing alopecia scarring lesions, and as well as in central centrifugal cicatricial alopecia. In the latter, a few remnants of hair follicles are visible, too. Areas of homogeneous dermis without structures are visible in traction alopecia at the cicatricial stage but with intact residual hairs, which helps to rule out other cicatricial alopecia [79].

Preprints.org (www.preprints.org) | NOT PEER-REVIEWED | Posted: 24 December 2024 doi:10.20944/preprints202412.1938.v1

In dissecting cellulitis subcutis echogenicity with a clear border outlines the inflamed area and can guide an intralesional steroid injection [79]. This disease presents similar findings with hidradenitis suppurativa, such as dilation of the hair follicles, anechoic or hypoechoic pseudocysts, fluid collections, and tunnels (also called fistulas) [80].

Folliculitis decalvans shows fusion of hair follicles, decreased dermal echogenicity and increased subcutaneous echogenicity [79].

Ultrasound can image trichilemmal cysts as dermal and/or subcutaneous oval-shaped heterogeneous hypoechoic lesions with inner echogenic material without a tract toward the epidermis, occasionally with few fragments of hair tracts and calcifications (Figure 15) [81].

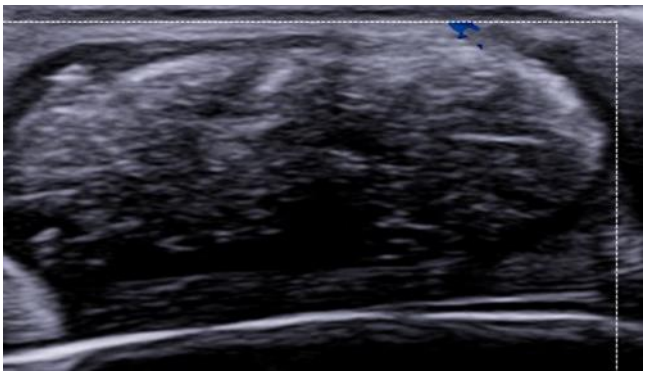

Figure 15. An oval dermal and subcutaneous heterogeneous hypoechogenic trichilemmal cyst in the scalp with keratinized material and hair fragment inside at 24 MHz.

Folliculotropic mycosis fungoides shows skin thickening, prominent upper dermis hypoechoic band due to lymphocytic infiltrates and some hyperechoic deposits around hair follicles because of mucin degeneration [82].

Scalp metastases are usually hypoechoic solid lesions with increased vascularity, and HFUS and UHFUS can rapidly and cost-effectively assess their size and sur-rounding anatomy; moreover, ultrasound can aid in directing subsequent imaging and treatment strategies, such as tissue sampling or surgical intervention [83].

Cutis verticis gyrata shows undulation of the cutaneous layers, dermal and hypodermal thickening, corresponding with the elevated clinical zones, followed by folds with normal cutaneous thicknesses [84].

UHFUS of vitiligo presents undulation of the epidermis, hypoechoic subepidermal thin plaques, hypoechoic and thickened regional hair follicles and/or pilosebaceous units with prominent sebaceous glands, as well as regional hypervascularity [85].

UHFUS can be used to assess the efficacy of a long-pulsed alexandrite laser for keratosis pilaris. In fact, four weeks after the fourth treatment, UHFUS demonstrated the flattening of the epidermal bulges, which were consistent with dermoscopic and histologic examinations [86].

HFUS can show pseudocysts, folliculitis, fistulas, calcinosis, and scars in acne patients and can help evaluate disease severity through the SOS-Acne (Figure 16). HFUS can identify acne scar depth and scar width (Figure 17); moreover, HFUS can assess treatment efficacy, such as Er:Yag laser therapy, after which a reduction of scar depth and epidermal thickness are reported. Moreover, CO2 fractional resurfacing laser treatment can be evaluated with HFUS, and dermal thickness measurement is suggested before treatment as a thick dermis seems less effectively treated than a thin one [87-91].

Preprints.org (www.preprints.org) | NOT PEER-REVIEWED | Posted: 24 December 2024 doi:10.20944/preprints202412.1938.v1

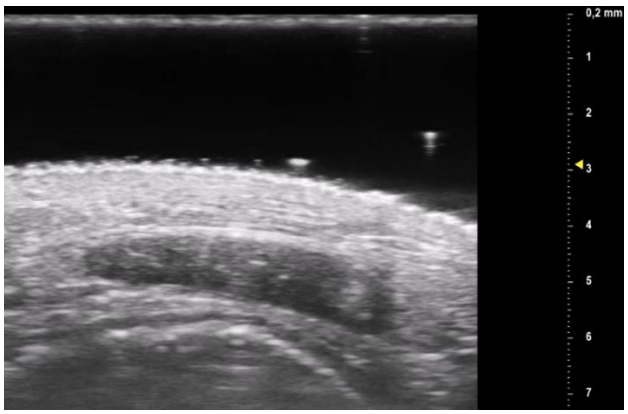

Figure 16. Acne pseudocyst at 70 MHz.

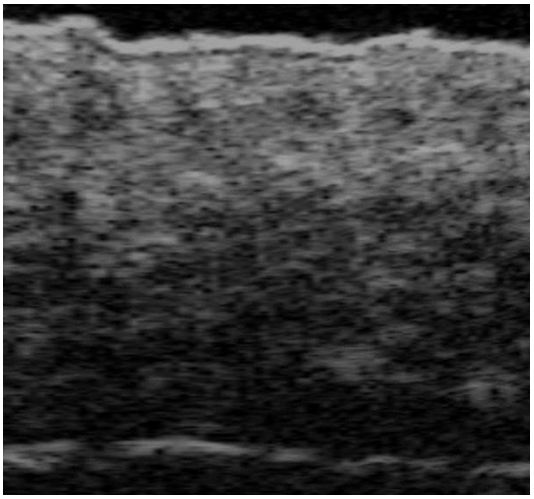

Figure 17. Forehead acne scar at 48 MHz**.**

Ultrasound helped prove the primary follicular involvement in hidradenitis suppurativa and allows us to assess subclinical disease and anatomical abnormalities clinically unrecognizable; therefore, baseline and follow-up ultrasound examinations are recommended [92]. UHFUS can detect drop-shaped hair follicles, micro-tunnels, and microcysts. HFUS can adequately evaluate fluid collections, abscesses, pseudocysts, location and morphology of tunnels allowing to correctly assess staging of severity (mSOS-HS) and scoring of activity (US-HSA), therefore assisting physicians in choosing the correct medical or surgical intervention and helping to predict treatment response, usually with scarce patient's discomfort (Figures 18–22) [93-98]. Moreover, UHFUS can guide intralesional steroid injection in HS flares that do not respond to topical treatment, and UHFUS can be used to assess therapeutic response [99, 100]. Presurgical lesion mapping by UHFUS is surely suggested in moderate and severe HS refractory to previous medical and surgical therapies, as UHFUS enables detailed assessment of lesion extension, particularly identifying tunnels and fistulas, facilitating surgical planning [101, 102]. Ultrasound can also evaluate associated or linked diseases, such as acne vulgaris, pilonidal sinus, dissecting cellulitis of the scalp, and perianal infective/inflammatory disease, and their treatment response (Figure 23) [103-108].

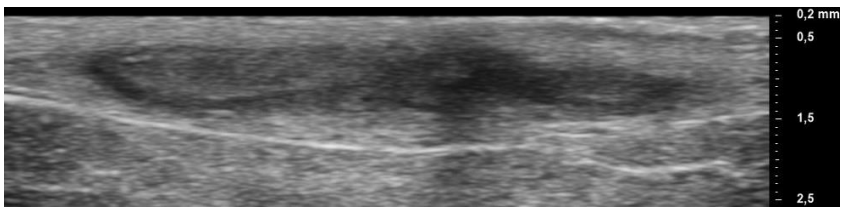

Preprints.org (www.preprints.org) | NOT PEER-REVIEWED | Posted: 24 December 2024 doi:10.20944/preprints202412.1938.v1

Figure 18. Hidradenitis suppurativa micro-tunnel at 70 MHz.

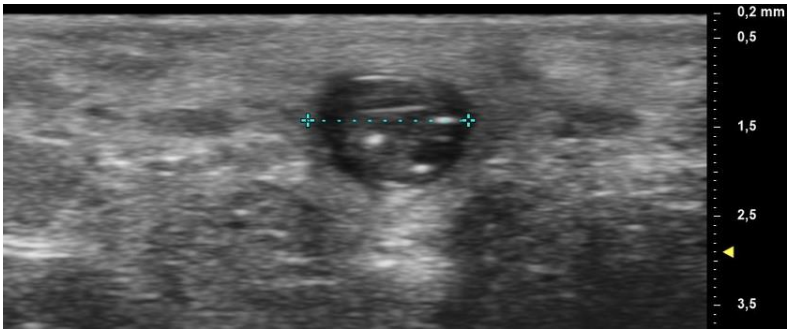

Figure 19. Hidradenitis suppurativa microcyst or ballooned hair follicle with 70 MHz probe.

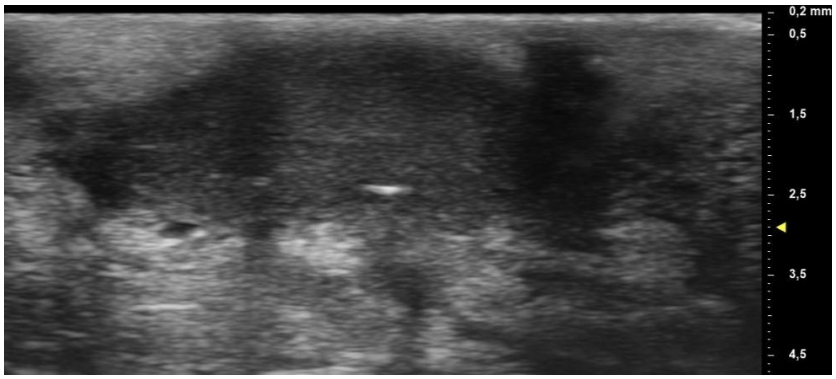

Figure 20. Hidradenitis suppurativa fluid collection at 70 MHz.

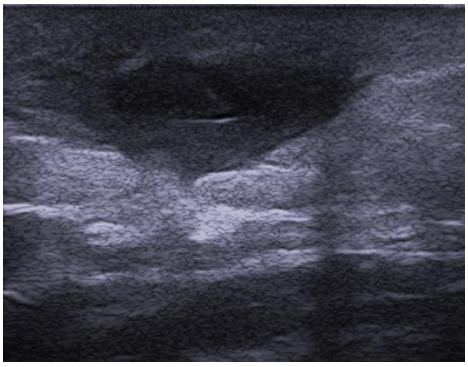

Figure 21. Grayscale 20MHz ultrasound image showing a subcutaneous fluid collection in the buttock of a patient with hidradenitis suppurativa. A retained hair fragment is visible as a linear hyperechoic structure within the abscess and aligned parallel to the skin surface.

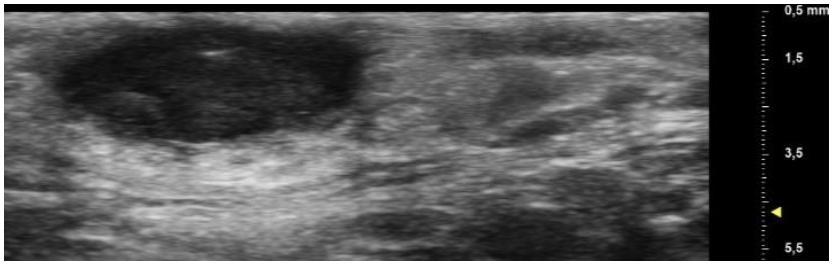

Figure 22. Hidradenitis suppurativa pseudocyst at 48 MHz.

Preprints.org (www.preprints.org) | NOT PEER-REVIEWED | Posted: 24 December 2024 doi:10.20944/preprints202412.1938.v1

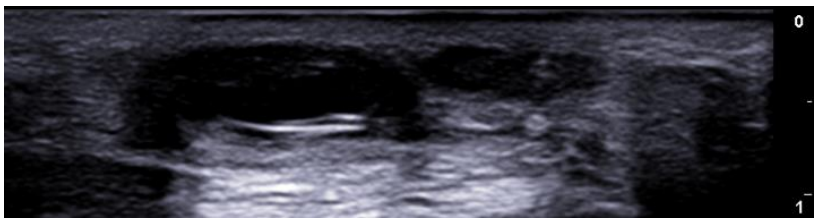

Figure 23. 24MHz ultrasound image showing a pilonidal sinus with hair fragments.

HFUS can help evaluate nail unit and nail plate thickness functions and diseases [109, 110].

Nail psoriasis can show thickened, hyperechoic, and wavy nail plates, with nail bed thickening and hypoechogenicity, focal hypoechoic deposits, and loss of definition in the ventral plate [111-116]; concomitant enthesopathy of the digital extensor tendon in the distal interphalangeal joint can be evaluated [117]. UHFUS can assess a decrease in the nail plate thickness after one month from the beginning of biologic treatment with mAb anti-TNF-alpha and anti-IL, even before clinical changes are detectable [118] (Figure 24).

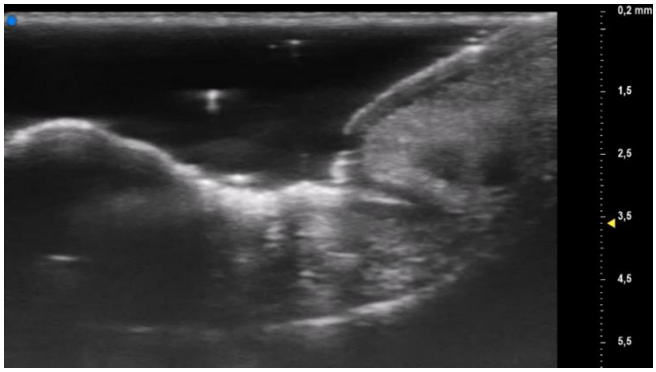

Figure 24. A 70MHz ultrasound image shows a thickened, hyperechoic, and wavy nail plate with an increased thickness of the nail bed in a patient with psoriasis.

Ultrasound can detect nail bed thickening, irregular thickening, and fusion of the nail plates in onychomycosis, and it can display periungual fold thickening, with areas of increased and decreased echogenicity, and increased vascularization in paronychia [119].

Onychopapilloma can be evaluated using HFUS, and matrix involvement evident on ultrasound imaging can help predict post-surgical recurrence. Onychopapilloma can present as a nail bed hypoechoic band, nail plate thickening, hyperechoic focal spots, upward displacement, and irregularities of the ventral plate [120].

Onychomadesis and retronychia can be evaluated well with HFUS, which can help identify defects under the proximal nail fold. Frequently, these conditions can be together. Onychomadesis is the fragmentation of the nail plate, and in retronychia a fragmented nail plate is commonly identified beneath the proximal nail fold. Signs of retronychia included a decreased distance between the origin of the nail plate and the base of the distal phalanx, thickening of the proximal nail fold, and a hypoechoic halo surrounding the origin of the nail plate; moreover, color-Doppler can detect hypervascularity areas and help decide if onychectomy is necessary [121] (Figure 25).

Preprints.org (www.preprints.org) | NOT PEER-REVIEWED | Posted: 24 December 2024 doi:10.20944/preprints202412.1938.v1

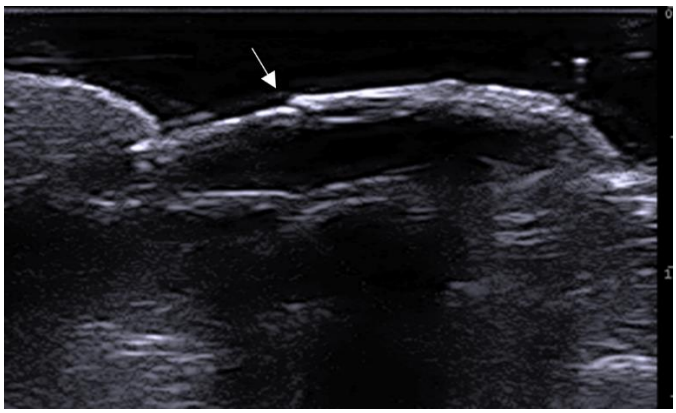

Figure 25. Longitudinal greyscale 20 MHz ultrasound of onychomadesis: note the abrupt interruption of the nail plate (arrow).

Nail lichen planus diagnosis can be supported by HFUS, avoiding potential permanent scars derived from nail biopsies; in fact, thickening, decreased echogenicity and hypervascularity of the nail bed can be detected, as well as a hypoechoic halo surrounding the origin of the nail plate in all or almost all fingers as well as thickening and decreased echogenicity of the periungual dermis; moreover, ultrasound can help monitor this disease's treatment [122].

HFUS can diagnose a subungueal glomus tumor, a benign tumor derived from the neuromyoarterial plexus. On ultrasound, it presents as an oval-shaped hypoechoic lesion with well-defined borders, intralesional hypervascularity at color Doppler, and bone cup-scalloping without cortical erosion [119, 123] (Figure 26).

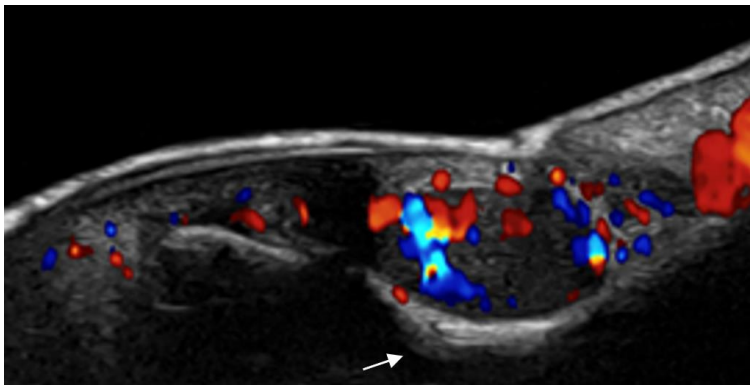

Figure 26. Glomus tumor of the right thumb at 24 MHz. Oval-shaped, well-defined, hypoechoic nodule that corresponds to a glomus tumor. There is hypervascularity within the tumor. Notice the scalloping of bony margin (arrow).

Ultrasound can be used to confirm the presence of a digital myxoid cyst (synovial cyst) and it is helpful to guide steroid injection and to follow-up lesion evolution after treatment; large digital myxoid cyst volume is associated with reduced prolonged cure rate, as well as osteophytes presence, older age, and long disease duration; these lesion characteristics can be evaluated to decide when directly offer surgical excision [124-126] (Figure 27).

Preprints.org (www.preprints.org) | NOT PEER-REVIEWED | Posted: 24 December 2024 doi:10.20944/preprints202412.1938.v1

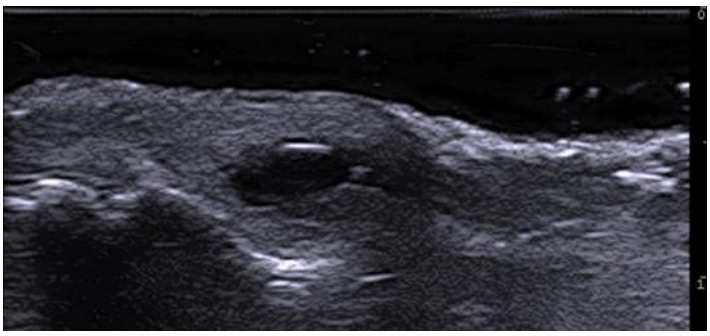

Figure 27. Longitudinal 20 MHz greyscale ultrasound of a digital myxoid cyst, showing a well-circumscribed anechoic lesion, with nail plate splitting due to compression on the matrix region and distal interphalangeal joint osteophytes.

Telangiectatic granuloma is a benign vascular tumor that usually appears as a hypoechoic, ill-defined, hypervascular dermal structure at the proximal nail fold without erosion of the nail plate or distal phalanx bony margin [127].

Squamous cell carcinoma is the most common nail apparatus malignancy and is a hypoechoic, hypervascular lesion with ill-defined margins, which causes nail plate and bony margin erosions [127].

In patients with longstanding melanonychia, ultrasound can help detect melanoma as ill-defined, hypoechoic, heterogeneous, and hypervascular structures or masses in the nail bed or matrix with nail plate and bone margin erosions [127].

In auricular and nasal non-melanoma skin cancer, preoperative HFUS can show deep cartilaginous or bone infiltration, thus resulting in radio-immunological treatment rather than surgery; in case of local cartilage infiltration, a more aggressive surgical procedure is performed, reducing the need for a second surgical intervention; when no depth infiltration is identified at ultrasound surgical excision is the treatment of choice [128].

Intraoral HFUS and UHFUS could help diagnose different oral pathologies and evaluate the depth of invasion and tumor thickness of persisting oral soft tissue lesions to predict adverse histological features preoperatively [129, 130].

In the case of congenital exclusively lingual pigmentation, epidermal choristoma can be differentiated by congenital lingual melanotic macule thanks to the demonstration at UHFUS of multiple hyperechoic oval-shaped submucosal structures, consistent with sebaceous glands, without hypervascularity [131].

6. Vascular Disorders

HFUS can be used to confirm capillary malformation diagnosis, follow-up the lesion, assist laser treatment, and evaluate treatment results. Moreover, HFUS can be useful to suspect the presence or diagnose clinically unexpected associated vascular malformation, such as arteriovenous malformations [132, 133] (Figure 27). Moreover, ultrasound can accurately and reliably diagnose intraneural vascular anomalies of peripheral nerves [134].

Preprints.org (www.preprints.org) | NOT PEER-REVIEWED | Posted: 24 December 2024 doi:10.20944/preprints202412.1938.v1

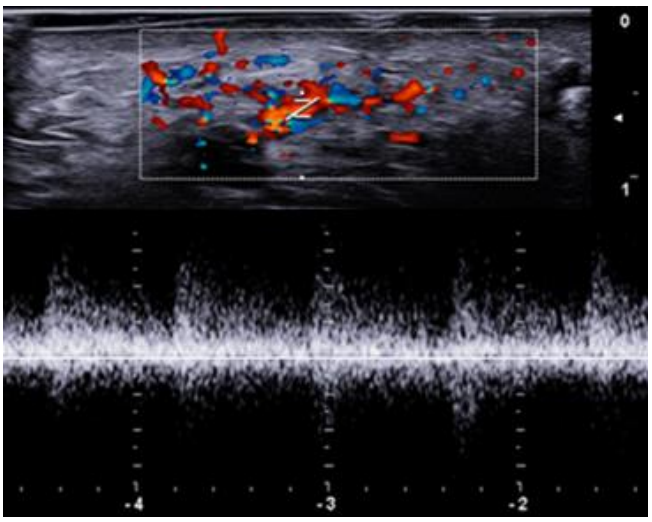

Figure 27. Left cheek vascular malformation with 24 MHz probe.

HFUS hypoechoic upper dermal hypoechogenicity thickness measurement can objectively assess edema severity and treatment adequacy in patients with venous ulcers, as it showed a significant reduction after compression therapy [135] (Figure 28).

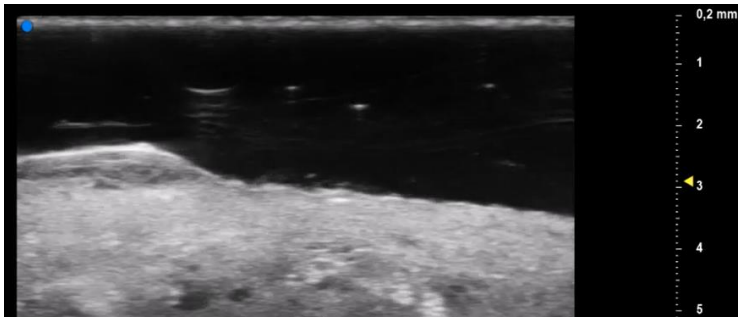

Figure 28. A 70MHz ultrasound image shows a venous ulcer with a decreased echogenicity band in the perilesional tissue.

High-frequency color Doppler ultrasound can help detect perforators in deep adipose layers before harvesting super-thin anterolateral thigh flap for the foot and ankle skin and soft tissue defects treatment after traffic accident, heavy object crush, mechanical and heat crush injuries to accurately detect perforators accurately located [136].

UHFUS allows us to detect more lymphatic vessels than conventional linear probe ultrasound, including lymphatics with diameters smaller than 0.3 mm that can show fluids moving inside the lymphatic lumen and may detect functioning valves. Identifying functional lymphatic vessels is very important for lymphedema cases preoperatively, as lymphaticovenular anastomosis is an effective and minimally invasive surgical treatment for refractory lymphedema [137]. In fact, UHFUS can be used to identify patient-oriented incisions for lymphaticovenular anastomosis in advanced-stage lymphedema as it helps to detect functioning lymphatic channels where it would have been considered impossible before [138, 139].

7. External Agents Associated Disorders

HFUS can non-invasively and objectively assess skin changes during radiotherapy [140, 141].

HFUS can evaluate epidermal and dermis thickness, epidermal oedema, dermal fibrosis, and follicle density in traumatic scars [142].

Ultrasound can be used to assess surgical wounds, as peri-incisional fluid collection detection is significantly associated with surgical site infection, suggesting a need for early therapy [143, 144].

Preprints.org (www.preprints.org) | NOT PEER-REVIEWED | Posted: 24 December 2024 doi:10.20944/preprints202412.1938.v1

HFUS can help distinguish between scarring, hypertrophic scars, and keloid, as hypertrophic scars show a striped hypoechoic area in the upper dermis. Keloids are characterized by a focal hypoechoic band with a laminar pattern extending beyond the scar's original site. In atrophic scars, the edges between dermis and subcutis are not well defined [145] (Figure 29).

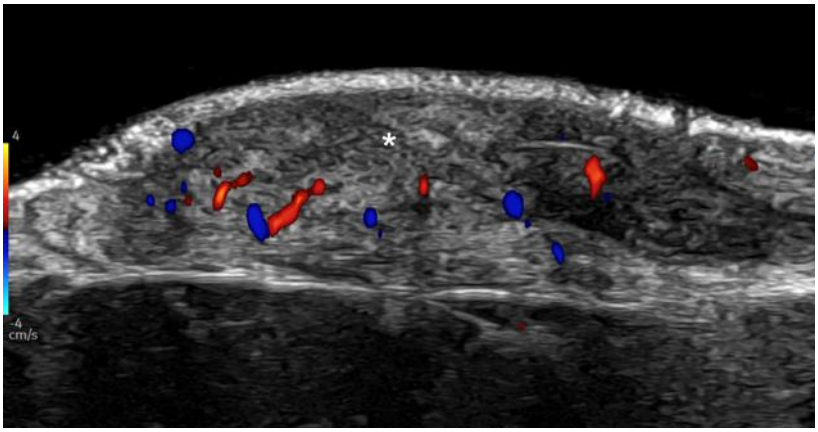

Figure 29. Active keloid. Hypoechoic laminar dermal thickening at 24 MHz that corresponds to a keloid (*). Notice the hypervascularity within the lesion.

HFUS can be used for leg ulcer imaging and healing process monitoring, such as after laser biostimulation of shin ulcers [146].

Ultrasound can detect radiolucent foreign bodies in extremities with high accuracy as hyperechoic structures, and UHFUS is a valuable tool for hand surgery; inert foreign bodies such as metal or glass generate a posterior acoustic reverberation; moreover, inflammation and granulomatous tissue in the periphery of a foreign body determine the frequent visualization of hypoechoic tissue around it [9, 26, 147, 148] (Figures 30 and 31).

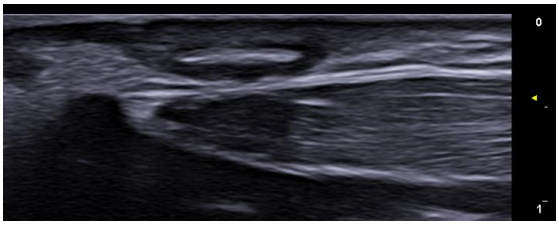

Figure 30. Garden cane fragment in the subcutis above the superficial head of first dorsal interosseous muscle of the right hand with **a** 24 MHz probe.

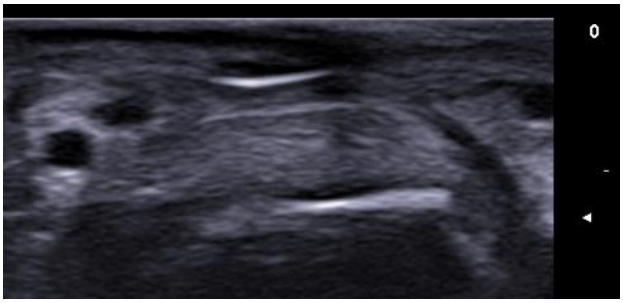

Figure 31. Glass fragment in the subcutis above the distal interphalangeal joint of the third finger with 24 MHz probe.

8. Neoplastic Diseases

Preprints.org (www.preprints.org) | NOT PEER-REVIEWED | Posted: 24 December 2024 doi:10.20944/preprints202412.1938.v1

HFUS is reported determine tumoral depth and locoregional staging of skin neoplasms useful for treatment planning, particularly for melanoma, basal cell carcinoma (BCC) and squamous cell carcinoma (SCC) [149-151]. Moreover, HFUS can diagnose local tumor recurrence as para-cicatricial or satellite masses (less than 2 cm from the primary tumor), in-transit metastases (equal or more than 2 cm from the primary tumor), and nodal metastases, also when not visible or not palpable. UHFUS can better detect small epidermal and/or upper dermal lesions. In addition, tumor recurrence mimickers can be adequately assessed in patients imaged for suspected tumor relapse. Furthermore, ultrasound-guided fine needle aspiration cytology of small suspected local recurrent tumors allows to perform the sampling precisely [152].

BCC and SCC are usually oval or band-like hypoechoic dermal and/or hypodermal vascularized structures; basal cell carcinoma commonly presents hyperechoic spots within the lesion, and a high-risk recurrent subtype lesion is suggested when seven or more hyperechoic spots are detected using a conventional linear probe at 15 MHz. These hyperechoic spots can be less visible or absent in superficial variants of BCC, and anechoic areas may be seen within adenoid-cystic BCC variants. Bowen disease, or squamous cell carcinoma in situ, can be evaluated with UHFUS and shows a wavy epidermal surface, hypoechogenicity of the lower part of the epidermis, and underlying dermis hypervascularity [153-157] (Figures 32–36).

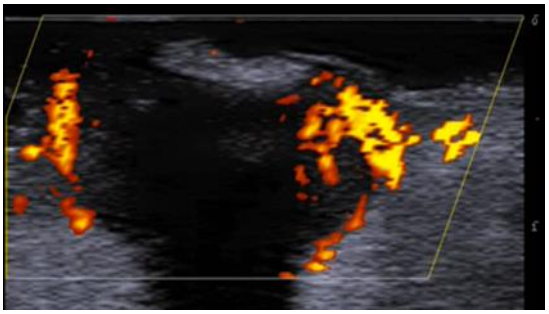

Figure 32. Power Doppler 20 MHz ultrasound image of an ulcerated nodular basal cell carcinoma of the preauricular area detects a well-defined, hypoechoic, round-shaped lesion with homogeneous echotexture, peripheral vascularity, andcalcification with acoustic shadowing.

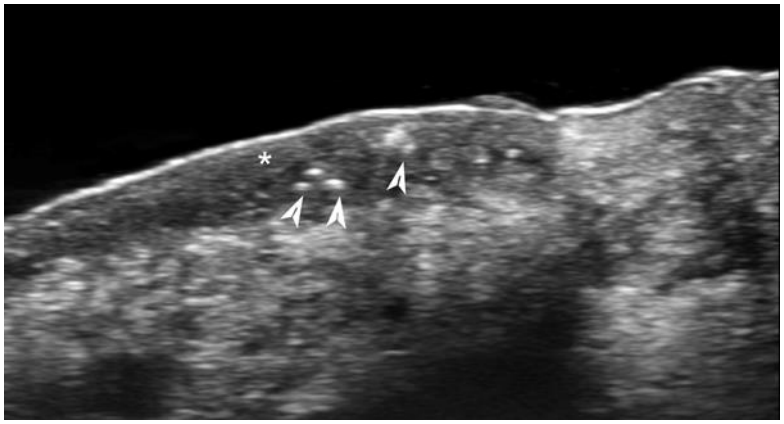

Figure 33. 70 MHz ultra-high-frequency ultrasound image of a hypoechoic subepidermal and dermal basal cell carcinoma. Notice the hyperechoic spots within the tumor (arrows).

Preprints.org (www.preprints.org) | NOT PEER-REVIEWED | Posted: 24 December 2024 doi:10.20944/preprints202412.1938.v1

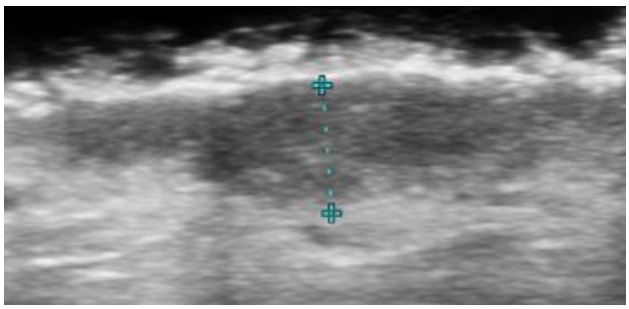

Figure 34. Hypoechoic subepidermal, dermal and dermo-hypodermal junction cheek superficial basal cell carcinoma at 48 MHz.

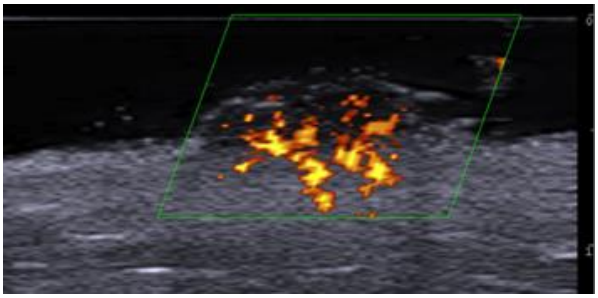

Figure 35. Power Doppler 20 MHz ultrasound image of an invasive G3 cutaneous squamous cell carcinoma reveals a hypoechoic, oval-shaped dermal mass with irregular borders, heterogeneous echotexture, and increased vascularity.

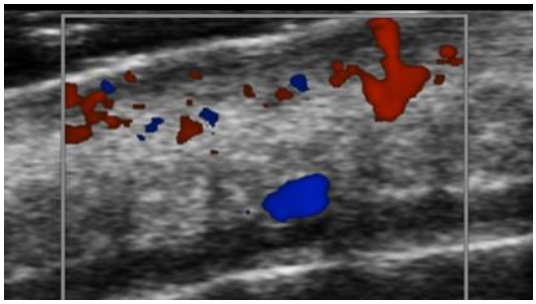

Figure 36. Color Doppler 48 MHz ultra-high-frequency ultrasound image of a hypoechoic in situ squamous cell carcinoma with mild mainly peripheral vascularization.

Melanomas frequently are dermal hypoechoic vascularized fusiform-shaped structures with peripheral inflammatory signs, such as decreased dermal echogenicity and increased subcutaneous echogenicity; in situ melanomas regular hyperechoic band between the lesion and the dermis can be showed by UHFUS; in flat lesions a well-circumscribed fusiform millimeter-sized tissue can be evaluated using UHFUS; ulcerated lesions can show epidermal irregularities and discontinuity; satellite lesions are hypoechoic oval, well-defined and vascularized masses; exophytic lesions shows hyperechoic epidermis with rough borders and hypoechoic tissue between the epidermis and dermis; moreover, ultrasound can detect local satellite recurrence or in-transit regional relapse; metastatic lymph nodes can show asymmetrical cortical thickening, hypoechoic or anechoic regions due to high cellularity, and chaotic cortical vascularity; what's more, ultrasound can guide lymph node cytology or biopsy [152, 157-162].

Merkel cell carcinoma presents as a hypoechoic richly vascularized dermal nodule that tends to invade subcutaneous tissue or deeper layers such as muscle or bone, frequently with posterior acoustic enhancement and epidermal thickening [163, 164].

UHFUS allows the assessment of imaging characteristics of primary cutaneous lymphomas, helping reach an accurate diagnosis and treatment response evaluation. Heterogeneous hypoechoic

Preprints.org (www.preprints.org) | NOT PEER-REVIEWED | Posted: 24 December 2024 doi:10.20944/preprints202412.1938.v1

nodules or pseudonodular lesions are more frequently reported in B-cell lymphomas instead of areas with dermal and/or hypodermal infiltration seem to be more commonly associated with T-cell lymphomas [157, 165, 166] (Figure 37); moreover, UHFUS can show epidermal thickness increase in patients with cutaneous T-cell lymphoma [167].

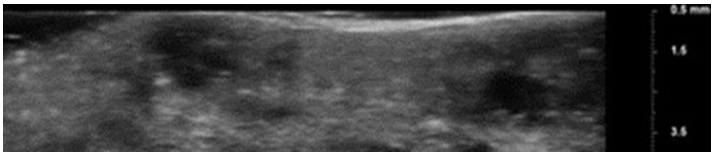

Figure 37. Two pseudonodular hypoechoic nose primary cutaneous B-cell lymphoma lesions at 48 MHz.

HFUS can provide clues for identifying cutaneous metastasis, as hypoechoic dermal and/or subcutaneous masses with ill-defined margins, irregular shape and vascularization can be observed in aggressive lesions [157, 168].

Cutaneous classic Kaposi sarcomas are usually hypoechoic, homogeneous, or heterogeneous and can go from avascular to hypervascular lesions. The avascular lesion can only require follow-up; instead, the lesions with internal vascular signals can require therapy as they are more prone to rapid clinical progression [169].

Pilomatrixomas, a benign tumor derived from the hair matrix, and dermatofibrosarcoma protuberans, a locally aggressive malignant fibrous tumor, have strong HFUS correlated findings. In fact, pilomatrixomas are usually well-defined dermal-hypodermal junction “target-type” lesions with an echogenic center, hyperechoic calcium spots within the nodule and hypoechoic rim [170] (Figure 38).

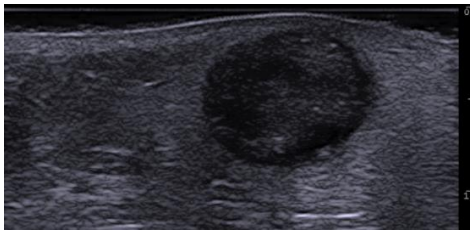

Figure 38. Grayscale 20 MHz ultrasound of a pilomatrixoma, showing a well-defined, round-shaped, mildly hypoechoic hypodermic mass with characteristic calcium spots and partial hypoechoic rim.

Dermatofibrosarcoma protuberans is described as an ill-defined oval hypoechoic dermal lesion with a hyperechoic hypodermal portion whit convex edges or tentacle-like projections, commonly vascularized on color Doppler. Recurrent dermatofibrosarcoma protuberans usually are oval or irregular-shaped, hypoechoic hypodermal masses [171, 172] (Figure 39).

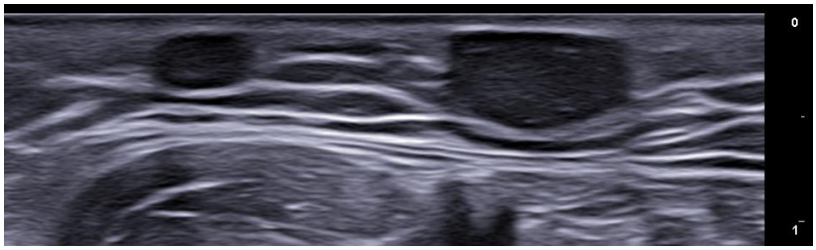

Figure 39. Subcutaneous dermatofibrosarcoma protuberans recurrent lesions with 24 MHz probe.

After biopsy and immunohistochemical analysis, preoperative sonography with subcutaneous infiltration identification can help diagnose pleomorphic dermal sarcoma instead of atypical fibroxanthoma, improving treatment strategy as resection with 2 cm safety margins and lymph node

Preprints.org (www.preprints.org) | NOT PEER-REVIEWED | Posted: 24 December 2024 doi:10.20944/preprints202412.1938.v1

sonography to rule out lymph node involvement is necessary for pleomorphic dermal sarcoma [173-175].

Cutaneous leiomyomatous tumors can be hypoechoic, pseudo-nodular, dermo-hypodermal structures with peripheral bundles, posterior acoustic reinforcement artifacts, and internal vascularity [176].

Infantile hemangiomas in the proliferative phase are hyper-vascularized hypoechoic masses with hyperechoic peripheral borders; the partial regression phase is characterized by less vascularity and mixed echogenicity; avascularity and hyper-echogenicity are usually reported in total regression phase sometimes associated with hypertrophic hypodermal lipodystrophy [177].

HFUS can help distinguish between dermatofibroma (or fibrous histiocytoma) high-risk and low-risk lesions; in fact, high-risk ones tend to be thicker with the subcutaneous component, irregularly shaped, heterogeneous and vascularized. Therefore, HFUS can be very useful for clinical management, as high-risk dermatofibromas need extensive surgical resection; instead, cryotherapy or laser treatment could be performed in low-risk lesions [178].

Other lesions in which ultrasound is very useful thanks to the very characteristic features are epidermal cysts, lipomas, schwannomas, and nodular fasciitis [81] (Figures 40–45).

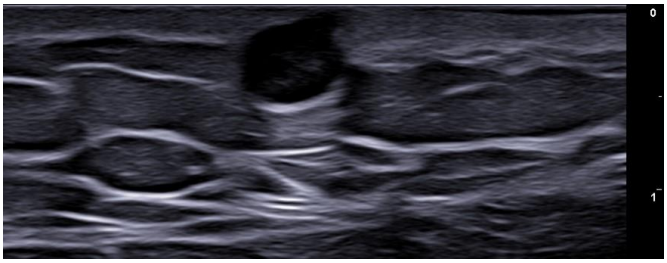

Figure 40. Dermo-epidermal hypoechoic round-shaped epidermal cyst with connecting tract toward the subepidermal and posterior enhancement at 24 MHz.

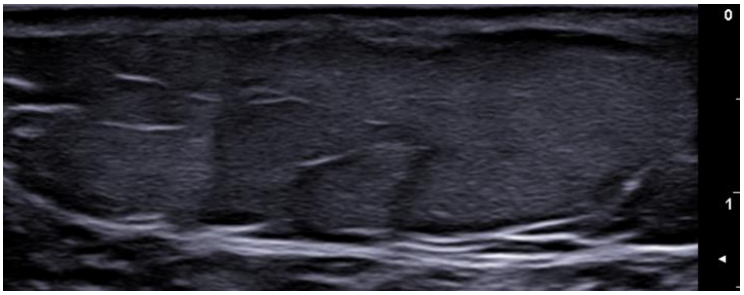

Figure 41. Mild hyperechoic oval-shaped lipoma of the left arm at 24 MHz.

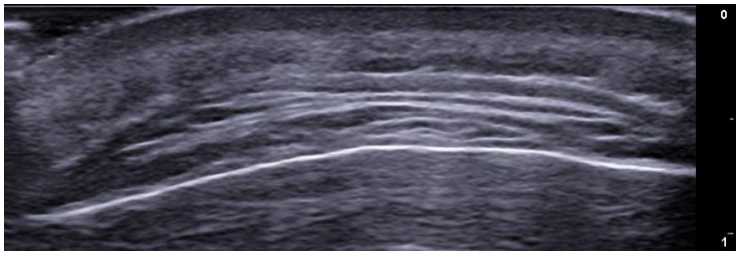

Figure 42. Well-defined hypoechoic subgaleal lipoma with hyperechoic septa between the frontalis muscle and the deep fascia at 24 MHz.

Preprints.org (www.preprints.org) | NOT PEER-REVIEWED | Posted: 24 December 2024 doi:10.20944/preprints202412.1938.v1

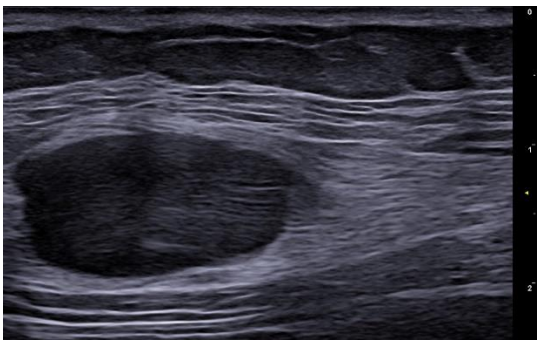

Figure 44. Well-delimited fusiform perifascial hypoechoic encapsulated schwannoma with mild posterior enhancement at 24 MHz.

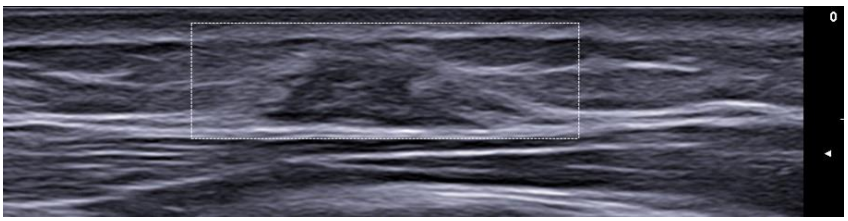

Figure 45. Irregular perifascial hypoechoic nodule with hyperechogenicity of the surrounding tissue because of edema, attached to the fascial layer in the deepest border representing nodular fasciitis at 24 MHz.

9. Aesthetic medicine

Ultra-high-frequency ultrasound helps assess surface area and length of fat protrusions at the dermal subcutaneous junction, as cellulite is characterized by discontinuous dermal–subcutaneous interface with papillae adiposae due to the presence of fibrous bands holding the dermis to the fascia; moreover, ultrasound can assess the effectiveness of anti-cellulite therapies [179-182] (Figures 46).

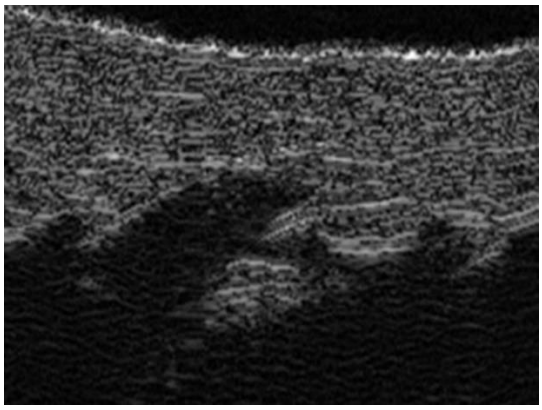

Figure 46. Cellulite at 50 MHz.

Dermal amount of water decreases during the aging process, and proteoglycans accumulate in the papillary dermis that determines the appearance of the subepidermal low echogenic band, whose thickness increases linearly with age in sun-exposed areas like the forehead, zygomatic region, and dorsal aspect of the forearm; therefore, subepidermal low echogenic band thickness is a valuable marker of photoaging [183, 184]

Aged skin reveals a thinner epidermis compared to younger skin, and HFUS can show epidermal thickening and upper dermis increased echogenicity three months after TCA-based anti-aging peeling [185, 186]

Preprints.org (www.preprints.org) | NOT PEER-REVIEWED | Posted: 24 December 2024 doi:10.20944/preprints202412.1938.v1

Twenty-four weeks after nasolabial fold dermal hyaluronic injection UHFUS can demonstrate increased dermal thickness and the percentage of wrinkle 3D fullness, providing valuable insight into the maintenance of results over time [187].

Temples, forehead, supraorbital region, glabella, tear trough, nasolabial groove, nose, lip, cheek, and chin facial filler materials can be well assessed using HFUS and UHFUS. In fact, hyaluronic acid, polyacrylamide, and lipofilling can show different ultrasound characteristics, echogenicity, fluidity, and blood flow signals. Anechoic well-defined pseudocystic deposits are typical for hyaluronic acid filler, whereas multiple thin strips of hypoechoic and anechoic areas, scattered in the hypoechoic loose subcutaneous tissue and other planes, may represent the spread and different injection technique of hyaluronic acid fillers [188, 189] (Figures 47 and 48).

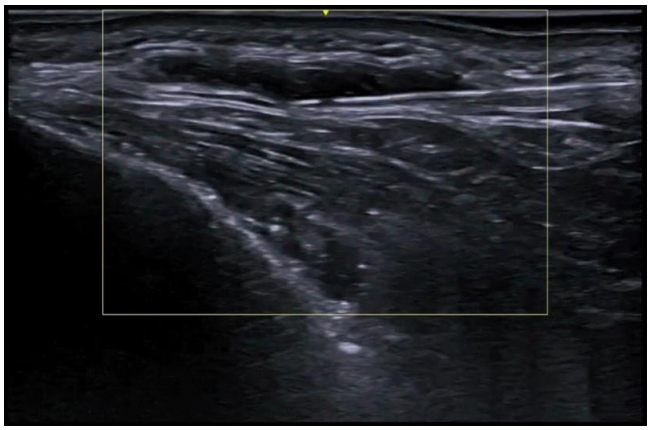

Figure 47. Temple hyaluronic acid filler injection at the interfascial plane (20 MHz).

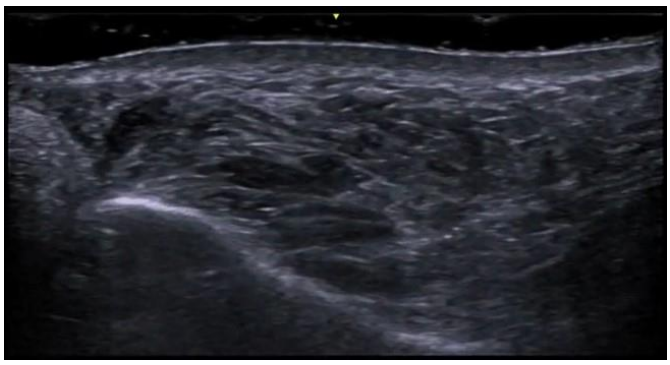

Figure 48. Sub-orbicularis oculi fat extensive deposits of hyaluronic acid, sagittal view at 20 MHz.

Anechoic pseudocystic structures that can contain echoes are suggestive of polyacrylamide. Iso-hypoechoic areas with some hyperechoic linear intervals are reported in transplanted fat. Hyperechoic deposits with posterior acoustic reverberance artifact, also called “snowstorm,” are suggestive of silicone oil. Undiluted calcium hydroxyapatite is represented by hyperechoic areas with strong posterior shadowing artifact; however, diluted presentations of calcium hydroxyapatite can present no posterior acoustic shadowing artifact. Hybrid fillers that combine calcium hydroxyapatite and hyaluronic acid are injected in the subcutaneous tissue and at HFUS are similar to calcium hydroxyapatite ones, but with lower posterior acoustic shadowing according to the dilution and mix with hyaluronic acid [188-190]. Polycaprolactone shows hypoechoic deposits with multiple bright hyperechoic spots with mini comet tail artifacts [191, 192]. Polymethylmethacrylate presents hyperechoic deposits with hyperechoic spots and mini comet tail artifacts with posterior acoustic shadow artifacts [193] (Figure 49).

Preprints.org (www.preprints.org) | NOT PEER-REVIEWED | Posted: 24 December 2024 doi:10.20944/preprints202412.1938.v1

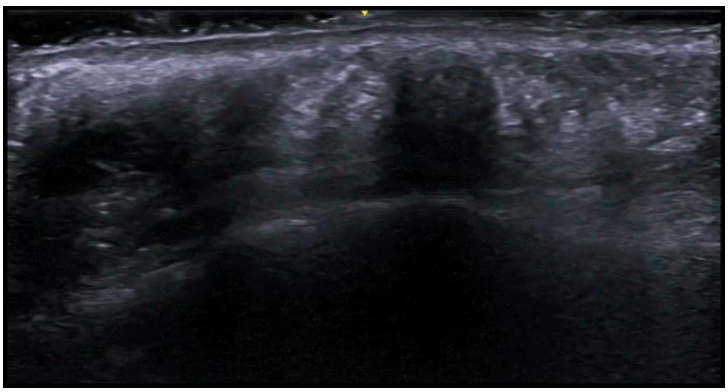

Figure 49. Prejowl sulcus polymethylmethacrylate at 20 MHz.

Facial and gluteal region microparticles of poly-l-lactic acid and carboxymethylcellulose hyperechoic deposits show posterior acoustic shadowing at the time of injection but not at follow-up two weeks later [191]. Silicone implants can be well-defined uniform anechoic structures (Figure 50).

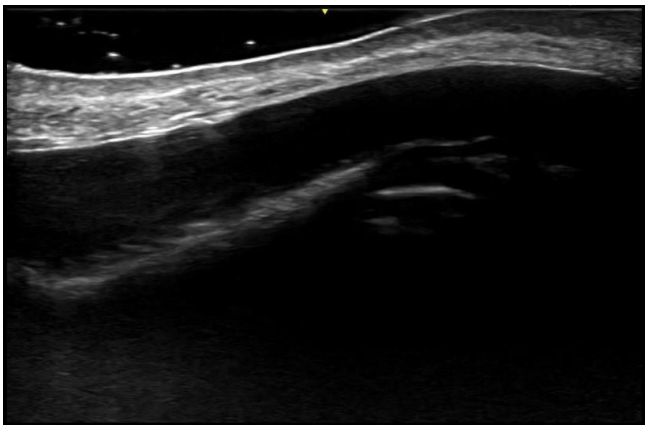

Figure 50. Nose silicone implant, sagittal view at 20 MHz.

HFUS can show dermal thickness increase and long-lasting correction of moderate to severe nasolabial folds at long-term follow-up following filler injection, possibly suggesting increase in collagen production after treatment [195-198].

In case of complications, inflammatory nodule shows increased blood flow signals on color-Doppler, with reduced echogenicity (Figure 51), and fat necrosis may manifest as an anechoic zone within subcutis. Some patients need additional filler injections after removing previous filling material and do not remember the exact type of material previously injected or inserted. HFUS can help distinguish these materials before re-treatment, helping avoid potential complications and identifying illegal fillers [188, 199-202].

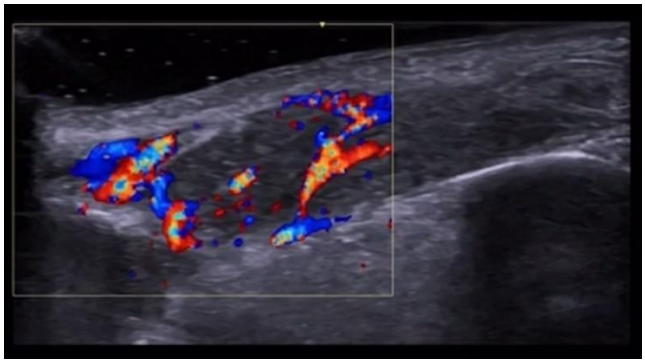

Figure 51. Color-Doppler image of infraorbital inflammatory hyaluronic acid nodule at 20 MHz.

Preprints.org (www.preprints.org) | NOT PEER-REVIEWED | Posted: 24 December 2024 doi:10.20944/preprints202412.1938.v1

HFUS is a valuable tool for aesthetic injectors as it allows the visualization of needle tip, arteries, and veins, increasing safety and ameliorating patients' outcomes. Vascular mapping using color-Doppler can be performed before and after procedures in high-risk face areas to reduce adverse events such as ischemia or tissue necrosis [203] (Figures 52–56).

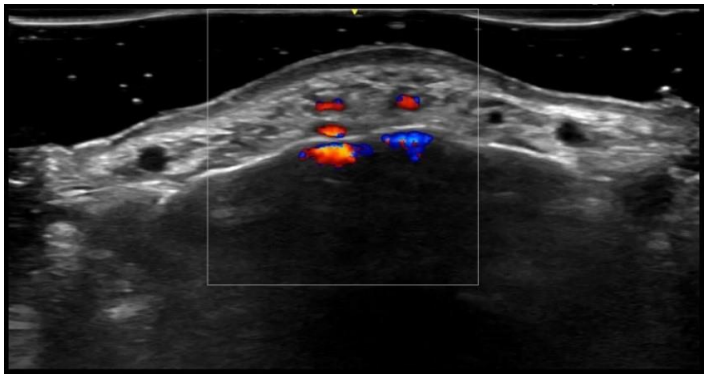

Figure 52. Color-Doppler image of multiple glabella arteries and veins at 20 MHz.

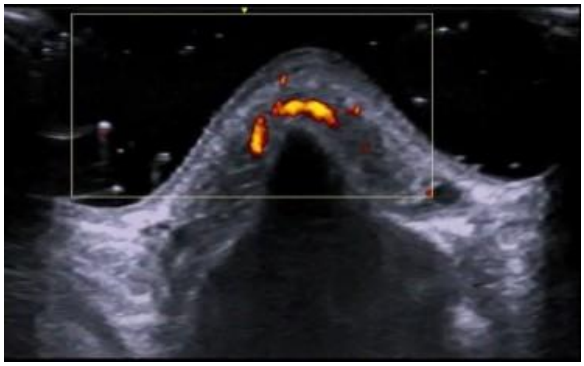

Figure 53. Color-Doppler image of nasal radix intercanthal vein at 20 MHz.

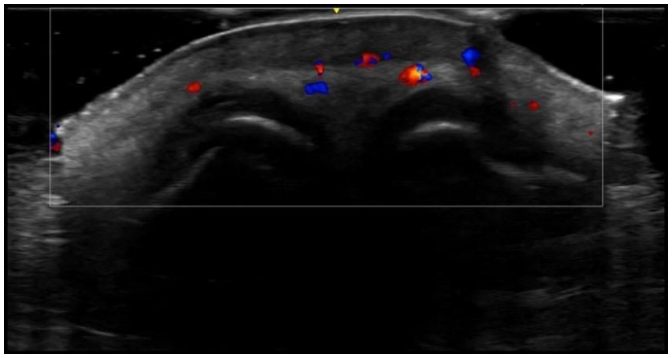

Figure 54. Color-Doppler image of nasal tip cartilage and multiple arteries at 20 MHz.

Preprints.org (www.preprints.org) | NOT PEER-REVIEWED | Posted: 24 December 2024 doi:10.20944/preprints202412.1938.v1

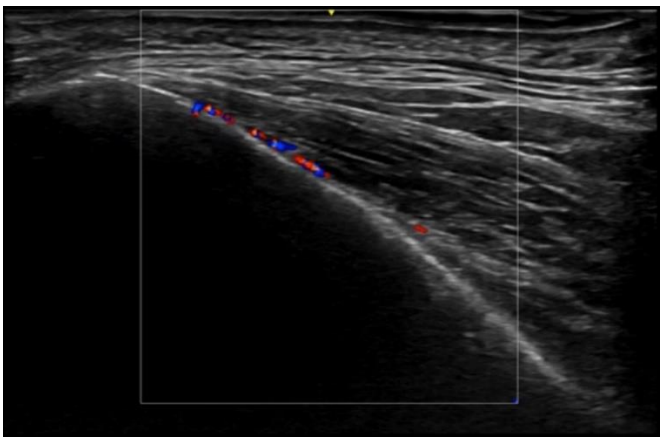

Figure 55. Color-Doppler image of the deep temporal artery at 20 MHz.

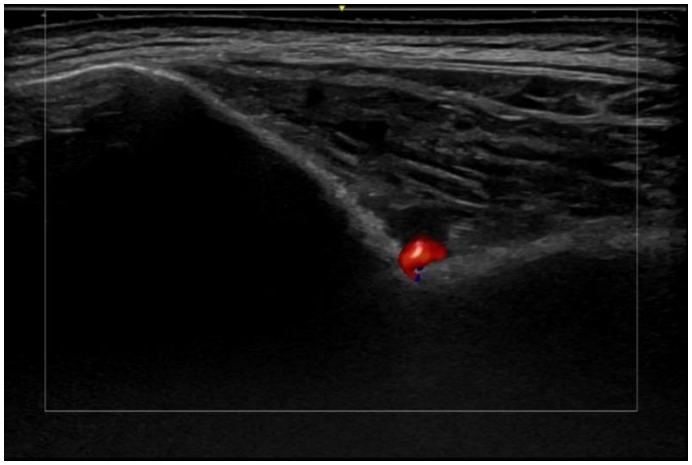

Figure 56. Color-Doppler image of the zygomaticotemporal artery at 24 MHz.

In case of vascular occlusion, including external compression, ultrasound-guided hyaluronidase application can be performed to reestablish vascular flow (Figures 57 and 58). Adjunctive use of self-administered 50% N_2O could help obtain relief of pain and anxiety and potentially additional perfusion improvement. Moreover, ultrasound can help evaluate filler migration, inflammatory reactions or infections [189, 203-212].

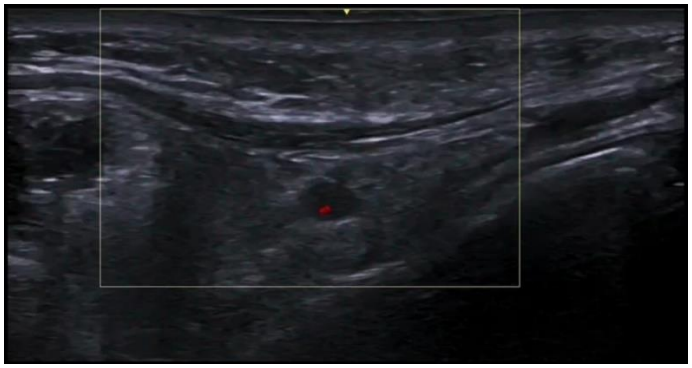

Figure 57. Facial artery near-occlusion at the mandible at 20 MHz.

Preprints.org (www.preprints.org) | NOT PEER-REVIEWED | Posted: 24 December 2024 doi:10.20944/preprints202412.1938.v1

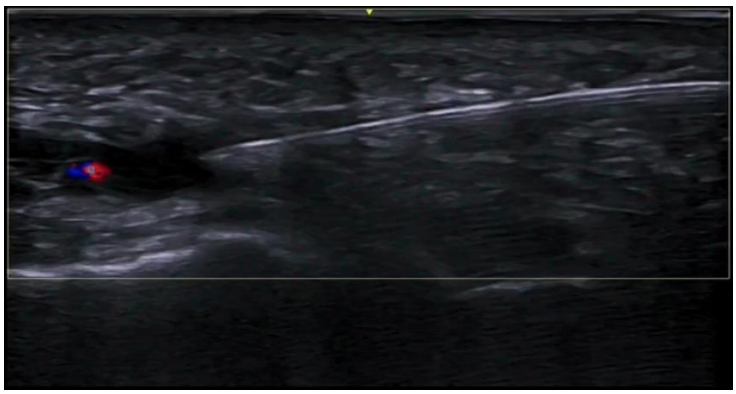

Figure 58. Angular artery with adjacent hyaluronic acid deposits: ultrasound-guided hyaluronidase injection in a case of vascular occlusion at 20 MHz.

A late complication of filler injection could be the appearance of palpable nodules, and HFUS helps distinguish between anechoic well-defined hyaluronic acid filler deposits and hypoechoic pseudonodules or areas suggestive of granulomas [213]. Moreover, fibrosis can demonstrate hyperechoic dermal and hypodermal areas with posterior acoustic shadowing [214]. Ultrasound can also guide intralesional drug injections of steroids, hyaluronidase, and 5-fluorouracil antimetabolite in case of difficult-to-treat foreign body granuloma reactions [215] (Figures 59–61).

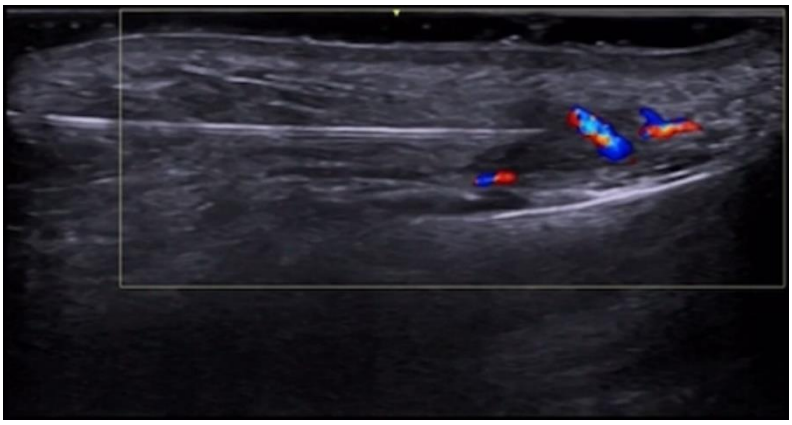

Figure 59. Ultrasound-guided hyaluronidase injection to an inflammatory infraorbital hyaluronic acid nodule.

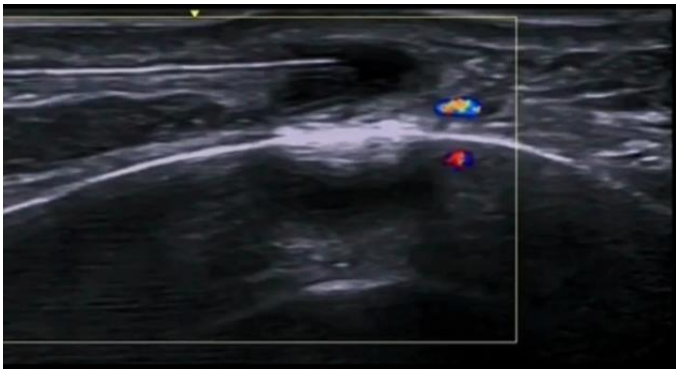

Figure 60. Hyaluronidase injection to the inflammatory prejowl hyaluronic acid nodule next to facial artery at 20 MHz.

Preprints.org (www.preprints.org) | NOT PEER-REVIEWED | Posted: 24 December 2024 doi:10.20944/preprints202412.1938.v1

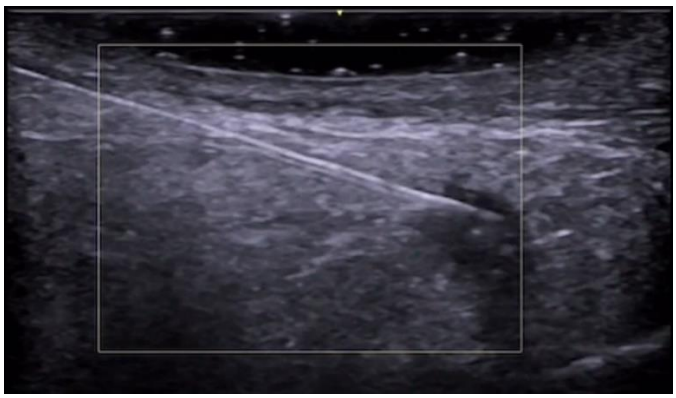

Figure 61. Hyaluronidase injection to retroseptal hyaluronic acid deposit at 20 MHz.

Granulomatous reaction secondary to fractional radiofrequency microneedling can show epidermal hypertrophy and dermal inflammation on ultrasound [216].

With regard to botulinum toxin applications, ultrasound can be performed before and during injection as muscle, tendons, and other structures can be easily visualized to improve efficacy and safety. Moreover, post-injection complications can be evaluated, such as lobular panniculitis, myositis, pseudoaneurysm, and asymmetric muscle contraction that can cause unwanted wrinkles or ptosis [217].

Finally, ultrasound can assess subcutaneous fat thickness and fat survival in gluteal fat grafting. The fat grafts appear as hypoechoic nodules with similar echogenicity compared to the subcutaneous tissue. Moreover, real-time use of ultrasound in gluteal fat transfer is becoming increasingly recommended to reduce complications, such as fat embolism, as ultrasound allows visualization of the transfer in the subcutaneous space, avoiding intramuscular injection [218-223]. Additionally, ultrasound can guide cannula positioning for liposuction [224].

10. Discussion

Dermatologists can evaluate the skin with different imaging modalities, and HFUS and UHFUS are increasingly being used as a complementary tool to clinical examination and dermoscopy to reach a correct diagnosis and to evaluate the best way to treat a disease or to evaluate treatment efficacy and duration [5, 225, 226].

In fact, for example HFUS's abilities to well evaluate cutaneous neoplasm size and depth are useful for procedural planning before surgical resection or radiotherapy, particularly in delineating accurate tumor margins and in areas where clinical inspection and dermoscopy are insufficient [5, 152, 227], and HFUS's capability to differentiate between a granuloma and a hyaluronic acid filler nodule is essential to decide the best treatment of an aesthetic procedure complication. If the clinical aspects of a cutaneous lesion are uncertain, ultrasound can contribute to diagnosing benign lesions, avoiding unnecessary surgery or advanced imaging studies such as MRI and CT, and planning specific topical or systemic treatments, which is obviously possible in pediatric patients, too [81, 228-230].

The fast-growing literature about HFUS and UHFUS demonstrates that these imaging modalities are already part of clinical dermatology practice and that this trend will tend to increase during the next years and decades, thanks to the diffusion of these new ultrasound machines and clinical expertise. Some barriers to dermatologic ultrasound were reported, but ultrasound education will certainly foster expanding future application of ultrasound in clinical practice [231-233].

Ultrasound imaging in skin diseases can be performed by dermatologists or other medical doctors who work strictly with dermatologists, such us radiologists; the latter eventuality could be particularly probable in large dermatological institutions in which radiologists with dermatoradiology expertise could also offer other imaging modalities when needed allowing better treatment and management of dermatology patients [234, 235]. Moreover, ultrasound imaging

Preprints.org (www.preprints.org) | NOT PEER-REVIEWED | Posted: 24 December 2024 doi:10.20944/preprints202412.1938.v1

utilization is growing among plastic surgeons in aesthetic medicine and reconstructive microsurgery fields [138, 208].

As regards future directions, the assessment of foreign body evaluation accuracy using high-frequency or ultra-high-frequency ultrasound compared to conventional linear probe ultrasonography could be performed in to evaluate the necessity to use this imaging modality in patients who need accurate and quick surgical resection to avoid complications and permanent pain due to incomplete removal. Another use that will probably expand with ultrasound is avoiding the need for serial biopsies in inflammatory conditions such as morphea or lichen planus. Future studies on rare malignancies, such as rare melanoma subtypes, are warranted based on the results of the more frequent types of melanomas. Moreover, the cost-effectiveness of these imaging modalities could be investigated to try to decide if the time to implement them in everyday clinical practice is arrived. More in-depth evaluation of the effects of anti-aging therapies or anti-cellulite treatments could be conducted in the future, and future research in to evaluate the usefulness of shear wave elastography could be performed. What's more, HFUS could be used to objectively assess human hypertrophic scar thickness variation after any surgical or invasive procedure such as botulinum toxin injections and, therefore, to evaluate its effect depending on different toxin concentrations [236].

11. Conclusions

HFUS and UHFUS are highly effective imaging modalities for skin evaluation, and their popularity in everyday clinical practice is constantly growing to assess skin diseases, plan procedures, monitor treatment efficacy and its duration, as well as to help diagnose and manage treatment complications such as in aesthetic procedures. In fact, they are already changing and will continue to modify dermatological everyday clinical practice as these new imaging modalities can be implemented to reach the best diagnosis, treatment, and management of skin diseases.

Author Contributions: Conceptualization, G.A., A.R. (Anna Russo), E.M., M.F., A.S., C.T., G.R., E.D.S., M.M., M.C., C.L., C.V., N.C., and V.P.; methodology, G.A., A.R. (Anna Russo), M.F., A.S., C.T., M.C., and G.R.; writing— original draft preparation, C.T., A.R. (Anna Russo), M.F., A.S., G.R., E.D.S., M.M., M.C., C.L., C.V., N.C., V.P., E.R., E.S.T., M.P., E.E:, G.L., G.L.P., C.G., F.P., A.R. (Alberto Rebonato), and G.M.G.; writing—review and editing, C.T., M.F., A.S., A.V.M., S.D., E.R., E.S., M.P., E.E., G.L., G.L.P., C.G., F.P., A.R. (Alberto Rebonato); supervision, A.R. (Alfonso Reginelli), A.V.M., S.D., G.M.G., A.O., S.C., and O.S. All authors have read and agreed to the published version of the manuscript.

Funding: This research received no external funding.

Institutional Review Board Statement: Not applicable.

Informed Consent Statement: Not applicable.

Data Availability Statement: Data is contained within the article.

Conflicts of Interest: The authors declare no conflict of interest.

References

1. Gaurav, V; Agrawal, S.; Najeeb, A.; Ahuja, R.; Saurabh, S.; Gupta, S. Advancements in Dermatological Imaging Modalities. *Indian Dermatol Online J.* **2024**;15:278-292.
2. Catalano, O.; Wortsman, X. Dermatology Ultrasound. Imaging Technique, Tips and Tricks, High-Resolution Anatomy. *Ultrasound Q*. **2020**;36:321-327.
3. Russo, A.; Reginelli, A.; Lacasella, G.V.; Grassi, E.; Karaboue, M.A.A.; Quarto, T.; Busetto, G.M.; Aliprandi, A.; Grassi, R.; Berritto, D. Clinical Application of Ultra-High-Frequency Ultra-sound. *J Pers Med*. **2022**;12:1733.

Preprints.org (www.preprints.org) | NOT PEER-REVIEWED | Posted: 24 December 2024 doi:10.20944/preprints202412.1938.v1

4. Mlosek, R.K.; Migda, B.; Migda, M. High-frequency ultrasound in the 21st century. *J Ultrason*. **2021**;20:e233-e241.
5. Crisan, D.; Wortsman, X.; Alfageme, F.; Catalano, O.; Badea, A.; Scharffetter-Kochanek, K.; Sindrilaru, A.; Crisan, M. Ultraso-nography in dermatologic surgery: revealing the unseen for improved surgical planning. *J Dtsch Dermatol Ges*. **2022**;20:913-926.
6. Wortsman, X. Practical applications of ultrasound in dermatology. *Clin Dermatol*. **2021**;39:605-623.
7. Rahmani, E.; Fayyazishishavan, E.; Afzalian, A.; Varshochi, S.; Amani-Beni, R.; Ahadiat, S.A.; Moshtaghi, Z.; Shafagh, S.G.; Khorram, R.; Asadollahzade, E.; et al. Point-Of-Care Ultrasonography for Identification of Skin and Soft Tissue Abscess in Adult and Pediatric Patients; a Systematic Review and Meta-Analysis. *Arch Acad Emerg Med*. **2023**;*11*:e49.
8. Barbic, D.; Chenkin, J.; Cho, D.D.; Jelic, T.; Scheuermeyer, F.X. In patients presenting to the emergency department with skin and soft tissue infections what is the diagnostic accuracy of point-of-care ultrasonography for the diagnosis of abscess compared to the current standard of care? A systematic review and meta-analysis. *BMJ Open*. **2017**;*7*:e013688.
9. Mese, I. Expanding dermatologic ultrasonography applications: further insights for enhanced patient management. *Ultrasonography*. **2023**;42:474-475.
10. Dominguez-Santas, M.; Roustan-Gullon, G.; Alfageme-Roldan, F. Sonographic findings in scabies. *J Ultrasound*. **2023**;26:549-551.
11. Wortsman, X.; Sazunic, I.; Jemec, G.B. Sonography of plantar warts: role in diagnosis and treatment. *J Ultrasound Med*. **2009**;28:787-793.
12. Corvino, A.; Catalano, O.; Wortsman, X.; Roldán, F.A.; Cavallieri, F.; Gonzalez, C.; Tafuri, D.; Corvino, F.; Cocco, G.; Caruso, M. High-Resolution Ultrasound of Odontogenic Cutaneous Sinus Tract: An International Multicentric Experience and a Review of the Literature. *J Ultrasound Med*. **2024**;43:1489-1499.
13. Giraldelli, G.A.; Baka, J.L.C.S.; Orofino-Costa, R.; Piñeiro-Maceira, J.; Barcaui, E.; Barcaui, C.B. In vivo reflectance confocal microscopy, dermoscopy, high-frequency ultrasonography, and histopathology features in a case of chromoblastomycosis. *PLoS Negl Trop Dis*. **2022**;16:e0010226.
14. Saavedra, A.C.; Valencia, B.M.; Tueros, P.; Wortsman, X.; Llanos-Cuentas, A.; Lavarello, R.J. Ultrasonographic characteristics of cutaneous leishmaniasis. *J Eur Acad Dermatol Venereol*. **2020**;34:e193-e195.
15. Vergara-de-la-Campa, L.; Cembrero-Saralegui, H.; Luna-Bastante, L.; Martínez-Lorenzo, E.R.; Alfageme-Roldán, F. Usefulness of ultrasound for treatment and follow-up of cutaneous leishmaniasis. *J Ultrasound*. **2021**;24:573-576.
16. Sechi, A.; Neri, I.; Patrizi, A.; Di Altobrando, A.; Clinca, R.; Caro, R.D.C.; Leuzzi, M.; Misciali, C.; Gaspari, V. Ultrasound patterns of localized cutaneous leishmaniasis and clinical correlations. *J Ultrasound*. **2022**;25:343-348.
17. Frade, M.A.; Nogueira-Barbosa, M.H.; Lugão, H.B.; Furini, R.B.; Marques Júnior, W.; Foss, N.T. New sonographic measures of peripheral nerves: a tool for the diagnosis of peripheral nerve involvement in leprosy. *Mem Inst Oswaldo Cruz*. **2013**;108:257–262.
18. Rao, P.N.; Suneetha, S. Pure neuritic leprosy: Current status and relevance. *Indian J Dermatol Venereol Leprol*. **2016**;82:252-261.
19. Voltan, G.; Marques-Júnior, W.; Santana, J.M.; Lincoln Silva, C.M.; Leite, M.N; De Paula, N.A., Bernardes Filho; F.; Barreto J.G.; Da Silva, M.B.; Conde, G.; et al. Silent peripheral neuropathy determined by high-resolution ultrasound among contacts of patients with Hansen's disease. *Front Med (Lausanne)*. **2023**;9:1059448.
20. Bouer, M.; Rodriguez-Bandera, A.I.; Albizuri-Prado, F.; Lobos, A.; Gubeling, W.; Wortsman, X. Real-time high-frequency colour Doppler ultrasound detection of cutaneous Dermatobia hominis myiasis. *J Eur Acad Dermatol Venereol*. **2016**;30:e180-e181.
21. Ogueta, I; Navajas-Galimany, L.; Concha-Rogazy, M.; Álvarez-Véliz, S.; Vera-Kellet, C.; Gonzalez-Bombardiere, S.; Wortsman, X. Very High- and High-Frequency Ultrasound Features of Cutaneous Larva Migrans. *J Ultrasound Med*. **2019**;38:3349-3358.
22. Wortsman, X. Sonography of Dermatologic Emergencies. *J Ultrasound Med*. **2017**;36:1905-1914.

Preprints.org (www.preprints.org) | NOT PEER-REVIEWED | Posted: 24 December 2024 doi:10.20944/preprints202412.1938.v1

23. Fan, W.; Zhang, Q.; Ye, X. High-frequency ultrasound findings in gonococcal inflammation of the paraurethral glands in men. *J Eur Acad Dermatol Venereol*. **2016**;30:146-147.
24. Fan, W.; Zhang, Q.; Ye, X.; Fan, Z. Dynamic Observation of the Morphological Changes in Paraurethral Ducts Infected with Gonococci in Men before and after Ceftriaxone Therapy Using High-Frequency Ultrasound. *Urol Int*. **2018**;100:240-244.
25. Negrutiu, M.; Danescu, S.; Popa, T.; Focsan, M.; Vesa, S.C.; Szasz, F.; Baican, A. Imaging Approach in the Diagnostics and Evaluation of the Psoriasis Plaque: A Preliminary Study and Literature Review. *Diagnostics (Basel)*. **2024**;14:969.
26. Wortsman, X. Re: Expanding dermatologic ultrasonography applications: further insights for enhanced patient management. *Ultrasonography*. **2023**;42:476-477.
27. Ianoși, S.L.; Forsea, A.M.; Lupu, M.; Ilie, M.A.; Zurac, S.; Boda, D.; Ianosi, G.; Neagoe, D.; Tutunaru, C.; Popa, C.M.; et al. Role of modern imaging techniques for the in vivo diagnosis of lichen planus. *Exp Ther Med*. **2019**;17:1052-1060.
28. Yazdanparast, T.; Yazdani, K.; Humbert, P.; Khatami, A.; Ahmad Nasrollahi, S.; Zartab, H.; Izadi Firouzabadi, L.; Firooz, A. Biophysical and ultrasonographic changes in lichen planus compared with uninvolved skin. *Int J Womens Dermatol*. **2018**;5:100-104.
29. Liu, Z.; Niu, Z.; Zhang, D.; Liu, J.; Zhu, Q. Improve the dupilumab therapy evaluation with dermoscopy and high-frequency ultrasound in moderate-to-severe atopic dermatitis. *Skin Res Technol*. **2023**;29:e13260.
30. Csány, G.; Gergely, L.H.; Kiss, N.; Szalai, K.; Lőrincz, K.; Strobel, L.; Csabai, D.; Hegedüs, I.; Marosán-Vilimszky, P.; Füzesi, K.; et al. Preliminary Clinical Experience with a Novel Optical-Ultrasound Imaging Device on Various Skin Lesions. *Diagnostics (Basel)*. **2022**;12:204.
31. Dini, V.; Iannone, M.; Michelucci, A.; Manzo Margiotta, F.; Granieri, G.; Salvia, G.; Oranges, T.; Janowska, A.; Morganti, R.; Romanelli, M. Ultra-High Frequency UltraSound (UHFUS) Assessment of Barrier Function in Moderate-to-Severe Atopic Dermatitis during Dupilumab Treatment. *Diagnostics (Basel)*. **2023**;13:2721.
32. Simonetti, O.; Bacchetti, T.; Ferretti, G.; Molinelli, E.; Rizzetto, G.; Bellachioma, L.; Offidani, A. Oxidative Stress and Alterations of Paraoxonases in Atopic Dermatitis. *Antioxidants (Basel)*. **2021**;10:697.
33. Zheng, X.; Wu, C.; Jin, H.; Liu, J.; Wang, H. Investigation of using very high-frequency ultrasound in the differential diagnosis of early-stage pemphigus vulgaris vs seborrheic dermatitis. *Skin Res Technol*. **2020**;26:476-481.
34. Molinelli, E.; Mancini, G.; Brisigotti, V.; Sapigni, C.; Simonetti, O.; Olivieri, A.; Offidani, A. Performance of high-frequency ultrasound in the evaluation of skin involvement in cutaneous chronic graft-versus-host disease: A preliminary report. *J Am Acad Dermatol*. **2022**;87:1180-1181.
35. Elsaiey, A.; Mahmoud, H.S.; Jensen, C.T.; Klimkowski, S.; Taher, A.; Chaudhry, H.; Morani, A.C.; Wong, V.K.; Salem, U.I.; Palmquist, S.M.; et al. Mastocytosis-A Review of Disease Spectrum with Imaging Correlation. *Cancers (Basel)*. **2021**;13:5102.
36. Białynicki-Birula, R.; Reszke, R.; Szepietowski, J.C. Two Ultrasonographic Patterns in Maculopapular Cutaneous Mastocytosis: A Preliminary Report. *Acta Dermatovenerol Croat*. **2017**;25:22-25.
37. Granieri, G.; Michelucci, A.; Manzo Margiotta, F.; Cei, B.; Vitali, S.; Romanelli, M.; Dini, V. The Role of Ultra-High-Frequency Ultrasound in Pyoderma Gangrenosum: New Insights in Pathophysiology and Diagnosis. *Diagnostics (Basel)*. **2023**;13:2802
38. Granieri, G.; Oranges, T.; Morganti, R.; Janowska, A.; Romanelli, M.; Manni, E.; Dini, V. Ultra-high frequency ultrasound detection of the dermo-epidermal junction: Its potential role in dermatology. *Exp Dermatol*. **2022**;31:1863-1871
39. Cheng, X.; Li, J.; Zhou, G.; Liu, Y.; Lu, X.; Wang, N.; Liu, H.; Zhang, F. High-Frequency Ultrasound in Blistering Skin Diseases: A Useful Method for Differentiating Blister Locations. *J Ultrasound Med*. **2017**;36:2367-2371.
40. Izzetti, R.; Nisi, M.; Aringhieri, G.; Vitali, S.; Oranges, T.; Romanelli, M.; Caramella, D.; Graziani, F.; Gabriele, M. Ultra-high frequency ultrasound in the differential diagnosis of oral pemphigus and pemphigoid: An explorative study. *Skin Res Technol*. **2021**;27:682-691.

Preprints.org (www.preprints.org) | NOT PEER-REVIEWED | Posted: 24 December 2024 doi:10.20944/preprints202412.1938.v1

41. Erew Chai, K.; Zhu, R.; Luo, F.; Shi, Y.; Liu, M.; Xiao, Y.; Xiao, R. Updated Role of High-frequency Ultrasound in Assessing Dermatological Manifestations in Autoimmune Skin Diseases. *Acta Derm Venereol*. **2022**;102:adv00765.
42. Ewrew Pu, Y.; Zhang, L. Application of dermatoscopy, reflectance confocal microscopy, and high-frequency ultrasound for diagnosing neonatal lupus erythematosus: A case report. *Skin Res Technol*. **2023**;29:e13291.
43. Chai, K.; Zhu, R.; Luo, F.; Shi, Y.; Liu, M.; Xiao, Y.; Xiao, R. Updated Role of High-frequency Ultrasound in Assessing Dermatological Manifestations in Autoimmune Skin Diseases. *Acta Derm Venereol*. **2022**;102:adv00765
44. Giavedoni, P.; Podlipnik, S.; Fuertes de Vega, I.; Iranzo, P.; Mascaró, J.M. Jr. High-Frequency Ultrasound to Assess Activity in Connective Tissue Panniculitis. *J Clin Med.* **2021**;10:4516
45. Romaní, J.; Giavedoni, P.; Roé, E.; Vidal, D.; Luelmo, J.; Wortsman, X. Inter- and Intra-rater Agreement of Dermatologic Ultrasound for the Diagnosis of Lobular and Septal Panniculitis. *J Ultrasound Med*. **2020**;39:107-112.
46. Svensson, C.; Eriksson, P.; Zachrisson, H.; Sjöwall, C. High-Frequency Ultrasound of Multiple Arterial Areas Reveals Increased Intima Media Thickness, Vessel Wall Appearance, and Atherosclerotic Plaques in Systemic Lupus Erythematosus. *Front Med (Lausanne).* **2020**;7:581336.
47. Leonard, D.; Akhter, T.; Nordmark, G.; Rönnblom, L.; Naessen, T. Increased carotid intima thickness and decreased media thickness in premenopausal women with systemic lupus erythematosus: an investigation by non-invasive high-frequency ultrasound. *Scand J Rheumatol*. **2011**;40:279-82.
48. Sudoł-Szopińska, I.; Żelnio, E.; Olesińska, M.; Gietka, P.; Ornowska, S.; Power, D.J.; Taljanovic, M.S. Update on Current Imaging of Systemic Lupus Erythematous in Adults and Juveniles. *J Clin Med*. **2022**;11:5212.
49. Kotob, H.; Kamel, M. Identification and prevalence of rheumatoid nodules in the finger tendons using high frequency ultrasonography. *J Rheumatol*. **1999**;26:1264-8.
50. Di Battista, M.; Barsotti, S.; Vitali, S.; Palma, M.; Granieri, G.; Oranges, T.; Aringhieri, G.; Dini, V.; Della Rossa, A.; Neri, E.; et al. Multiparametric Skin Assessment in a Monocentric Cohort of Systemic Sclerosis Patients: Is There a Role for Ultra-High Frequency Ultrasound? *Diagnostics (Basel).* **2023**;13:1495.
51. Daoudi, K.; Kersten, B.E.; van den Ende, C.H.M.; van den Hoogen, F.H.J.; Vonk, M.C.; de Korte, C.L. Photoacoustic and high-frequency ultrasound imaging of systemic sclerosis patients. *Arthritis Res Ther*. **2021**;23:22.
52. Di Battista, M.; Vitali, S.; Barsotti, S.; Granieri, G.; Aringhieri, G.; Morganti, R.; Dini, V.; Della Rossa, A.; Romanelli, M.; Neri, E.; et al. Ultra-high frequency ultrasound for digital arteries: improving the characterization of vasculopathy in systemic sclerosis. *Semin Arthritis Rheum*. **2022**;57:152105.
53. Yazdanparast, T.; Mohseni, A.; Dehghan, K.S.; Delavar, S.; Firooz, A. High-frequency ultrasound evaluation of morphea: Retrospective analytical study. *Skin Res Technol.* **2024**;30:e13818
54. Ranosz-Janicka, I.; Lis-Święty, A.; Skrzypek-Salamon, A.; Brzezińska-Wcisło, L. An extended high-frequency ultrasound protocol for assessing and quantifying of inflammation and fibrosis in localized scleroderma. *Skin Res Technol*. **2019**;25:359-366.
55. Khorasanizadeh, F.; Kalantari, Y.; Etesami, I. Role of imaging in morphea assessment: A review of the literature. *Skin Res Technol.* **2023**;29:e13410.
56. Etesami, I.; Azizi, N.; Sabrinejad, R.; Montazeri, S.; Kamyab, K.; Nasimi, M.; Mahmoudi, H.; Khorasanizadeh, F.; Wortsman, X. Sonographic skin features and shear wave elastography in distinguishing active from inactive morphea lesions: A case-control study. *J Am Acad Dermatol*. **2024**:S0190-9622(24)02877-9.
57. Wortsman, X.; Wortsman, J.; Sazunic, I.; Carreño, L. Activity assessment in morphea using color Doppler ultrasound. *J Am Acad Dermatol*. **2011**;65:942-8.
58. Wortsman, X. Role of Color Doppler Ultrasound in Cutaneous Inflammatory Conditions. *Semin Ultrasound CT MR*. **2024**;45:264-286.
59. Parra-Cares. J.; Wortsman, X.; Alfaro-Sepúlveda, D.; Mellado-Francisco, G.; Ramírez-Cornejo, C.; Vera-Kellet, C. Color Doppler Ultrasound Assessment of Subclinical Activity With Scoring of Morphea. *J Cutan Med Surg*. **2023**;27:454-460.

Preprints.org (www.preprints.org) | NOT PEER-REVIEWED | Posted: 24 December 2024 doi:10.20944/preprints202412.1938.v1

60. Wortsman, X.; Vera-Kellet, C. Ultrasound Morphea Activity Scoring (US-MAS): Modified US-MAS. *J Ultrasound Med*. **2023**;42:2447-2450.
61. Vera-Kellet. C.; Meza-Romero, R.; Moll-Manzur, C.; Ramírez-Cornejo, C.; Wortsman, X. Low effectiveness of methotrexate in the management of localised scleroderma (morphea) based on an ultrasound activity score. *Eur J Dermatol*. **2021**;31:813-821.
62. Araneda-Ortega, P.; Poblete-Villacorta, M.J.; Muñoz-López, C.; Vera-Kellet, C.; Wortsman, X. Morphea After Liposuction Ultrasonography. *J Ultrasound Med*. **2022**;41:2629-2635.
63. Noe, M.H.; Rodriguez, O.; Taylor, L.; Sultan, L.; Sehgal, C.; Schultz, S.; Gelfand, J.M.; Judson, M.A.; Rosenbach, M. High frequency ultrasound: a novel instrument to quantify granuloma burden in cutaneous sarcoidosis. *Sarcoidosis Vasc Diffuse Lung Dis*. **2017**;34:136-141.
64. Rodriguez, O.; Noe, M.H.; Sehgal, C.; Schultz, S.; Rosenbach, M. Quantification of granuloma volume and response to treatment in cutaneous sarcoidosis using 3-dimensional high-frequency ultrasound scan. *JAAD Case Rep*. **2017**;3:522-523.
65. Planas-Ciudad, S.; Roé Crespo, E.; Mir-Bonafé, J.F.; Muñoz-Garza, F.Z.; Puig Sanz, L. Dystrophic Calcification in a Patient with Primary Localized Cutaneous Nodular Amyloidosis: An Uncommon Ultrasound Finding. *Acta Derm Venereol.* **2018**;98:144-145.
66. García-Arpal, M.; Bujalance-Cabrera, C.; Banegas-Illescas, M.E.; Sánchez-Caminero, M.P.; González-Ruiz, L.; Villasanti-Rivas, N. Scleredema diabeticorum in a patient: un uncommon etiology of restrictive lung pattern Escleredema diabeticorum en un paciente: una etiología infrecuente de patrón restrictivo pulmonar. *Dermatol Online J.* **2021**;27:13030/qt71g4k3qf
67. Shih, S.R.; Lin, M.S.; Li, H.Y.; Yang, H.Y.; Hsiao, Y.L.; Chang, M.T.; Chen, C.M.; Chang, T.C. Observing pretibial myxedema in patients with Graves' disease using digital infrared thermal imaging and high-resolution ultrasonography: for better records, early detection, and further investigation. *Eur J Endocrinol.* **2011**;164:605-11.
68. Elahmar, H.; Feldman, B.M.; Johnson, S.R. Management of Calcinosis Cutis in Rheumatic Diseases. *J Rheumatol.* **2022**;49:980-989.
69. Tubau, C.; Cubiró, X.; Amat-Samaranch, V.; Garcia-Melendo, C.; Puig, L.; Roé-Crespo, E. Clinical and ultrasonography follow-up of five cases of calcinosis cutis successfully treated with intralesional sodium thiosulfate. *J Ultrasound*. **2022**;25:995-1003.
70. Mohafez, H.; Ahmad, S.A.; Hadizadeh, M.; Moghimi, S.; Roohi, S.A.; Marhaban, M.H.; Saripan, M.I.; Rampal, S. Quantitative assessment of wound healing using high-frequency ultrasound image analysis. *Skin Res Technol*. **2018**;24:45-53.
71. Chao, C.Y.; Zheng, Y.P.; Cheing, G.L. The association between skin blood flow and edema on epidermal thickness in the diabetic foot. *Diabetes Technol Ther.* **2012**;14:602-609.
72. Chao, C.Y.; Zheng, Y.P.; Cheing, G.L. Epidermal thickness and biomechanical properties of plantar tissues in diabetic foot. *Ultrasound Med Biol.* **2011**;37:1029-1038.
73. Wang, T.; Wang, Y.; Dong, Q.; Xu, C.; Zhou, X.; Ouyang, Y.; Liu, Y.; Lee, J.J.; Hu, N.; Wang, K.; et al. X-linked dominant protoporphyria in a Chinese pedigree reveals a four-based deletion of ALAS2. *Ann Transl Med*. **2020**;8:344.
74. Goldberg, I.; Sprecher, E.; Schwartz, M.E.; Gaitini, D. Comparative study of high-resolution multifrequency ultrasound of the plantar skin in patients with various types of hereditary palmoplantar keratoderma. *Dermatology*. **2013**;226:365-370
75. Guérin-Moreau, M.; Leftheriotis, G.; Le Corre, Y.; Etienne, M.; Amode, R.; Hamel, J.F.; Croué, A.; Le Saux, O.; Machet, L.; Martin, L. High-frequency (20-50 MHz) ultrasonography of pseudoxanthoma elasticum skin lesions. *Br J Dermatol*. **2013**;169:1233-1239.
76. Mikiel, D.; Polańska, A.; Żaba, R.; Adamski, Z.; Dańczak-Pazdrowska, A. Suitability of high-frequency ultrasonography (20 MHz) in evaluation of various forms of primary cicatricial alopecia in relation to trichoscopy - pilot study. *Skin Res Technol*. **2021**;27:774-784.
77. Mikiel, D.; Polańska, A.; Żaba, R.; Adamski, Z.; Dańczak-Pazdrowska, A. Usefulness of high-frequency ultrasonography in the assessment of alopecia areata - comparison of ultrasound images with trichoscopic images. *Postepy Dermatol Alergol*. **2022**;39:132-140.

Preprints.org (www.preprints.org) | NOT PEER-REVIEWED | Posted: 24 December 2024 doi:10.20944/preprints202412.1938.v1

78. Paun, M.; Tiplica, G.S. Non-Invasive Techniques for Evaluating Alopecia Areata. *Maedica (Bucur)*. **2023**;18:333-341
79. Kinoshita-Ise, M.; Ohyama, M.; Ramjist, J.M.; Foster, F.S.; Yang, V.X.D.; Sachdeva, M.; Sade, S.; Shear N.H. Ultra high-frequency ultrasound with seventy-MHz transducer in hair disorders: Development of a novel noninvasive diagnostic methodology. *J Dermatol Sci*. **2021**;102:167-176.
80. Cataldo-Cerda, K.; Wortsman, X. Dissecting Cellulitis of the Scalp Early Diagnosed by Color Doppler Ultrasound. *Int J Trichology*. **2017**;9:147-148.
81. Zattar, L.; Wortsman, X. Ultrasound of Benign Cutaneous Tumors and Pseudotumors: The Key Lesions. Semin Ultrasound CT MR. 2024;45:192-215.
82. Wortsman, X.; Wortsman, J.; Matsuoka, L.; Saavedra, T.; Mardones, F.; Saavedra, D.; Guerrero, R.; Corredoira, Y. Sonography in pathologies of scalp and hair. *Br J Radiol*. **2012**;85:647-655.
83. Cedirian, S.; Rapparini, L.; Sechi, A.; Piraccini, B.M.; Starace, M. Diagnosis and Management of Scalp Metastases: A Review. *Diagnostics (Basel)*. **2024**;14:1638.
84. Ortiz-Orellana, G.; Ferreira-Wortsman, C.; Wortsman, X. Ultrasound Pattern of Cutis Verticis Gyrata. *J Ultrasound Med*. **2024** Feb;43(2):405-409.
85. Wortsman, X.; Araya, I.; Maass, M.; Valdes, P.; Zemelman, V. Ultrasound Patterns of Vitiligo at High Frequency and Ultra-High Frequency. *J Ultrasound Med*. **2024**;43:1605-1610.
86. Li, M.; Bai, Y.; Duan, Z.; Yuan, R.; Liu, X.; Liu, Y.; Liang, X.; Wu, H.; Zhuo, F. Efficacy and Safety of Long-Pulsed 755-nm Alexandrite Laser for Keratosis Pilaris: A Split-Body Randomized Clinical Trial. Dermatol Ther (Heidelb). **2022**; 12:1897-1906.
87. Wortsman, X.; Claveria, P.; Valenzuela, F.; Molina, M.T.; Wortsman, J. Sonography of acne vulgaris. *J Ultrasound Med*. **2014**;33:93-102.
88. Tao, Y.; Wei, C.; Su, Y.; Hu, B.; Sun, D. Emerging High-Frequency Ultrasound Imaging in Medical Cosmetology. *Front Physiol*. **2022**;13:885922.
89. Malinowska, S.; Jaguś, D.; Woźniak, W.; Mlosek, R.K. Usefulness of high-frequency ultrasound in the monitoring of laser treatment of acne scars. *J Ultrason*. **2021**;20:e279-e283.
90. Naouri, M.; Atlan, M.; Perrodeau, E.; Georgesco, G.; Khallouf, R.; Martin, L.; Machet, L. High-resolution ultrasound imaging to demonstrate and predict efficacy of carbon dioxide fractional resurfacing laser treatment. *Dermatol Surg*. **2011;**37:596-603.
91. Ñanco-Meléndez, C.; Yagnam-Díaz, M.; Muñoz-Cáceres, M.; Contador-González, J.; Gubelin-Harcha, W.; Chicao-Carmona, F.; Tan, J.; Wortsman, X. Evaluation of Ultrasound Changes With the Use of Microneedling Versus Fractional CO2 Laser in Atrophic Acne Scars. *Dermatol Pract Concept*. **2024**;14:e2024168.
92. Reyes-Baraona, F.; Herane, M.I.; Wortsman, X.; Figueroa, A.; García-Huidobro, I.; Giesen, L.; Kolbach, M.; Molina, M.T.; Muñoz, L.; Saavedra, D.; et al. Chilean clinical guideline for the management of hidradenitis suppurativa - executive summary. *Rev Med Chil*. **2021**;149:1620-1635.
93. Wortsman, X. Update on the role of color Doppler ultrasound in hidradenitis suppurativa: a game-changer. *Ital J Dermatol Venerol*. **2024** Nov 19. doi: 10.23736/S2784-8671.24.08025-3. Epub ahead of print
94. Oranges, T.; Vitali, S.; Benincasa, B.; Izzetti, R.; Lencioni, R.; Caramella, D.; Romanelli, M.; Dini, V. Advanced evaluation of hidradenitis suppurativa with ultra-high frequency ultrasound: A promising tool for the diagnosis and monitoring of disease progression. *Skin Res Technol*. **2020**;26:513-519.
95. Wortsman, X.; Calderon, P.; Castro, A. Seventy-MHz Ultrasound Detection of Early Signs Linked to the Severity, Patterns of Keratin Fragmentation, and Mechanisms of Generation of Collections and Tunnels in Hidradenitis Suppurativa. *J Ultrasound Med*. **2020**;39:845-857.
96. Wortsman, X. Update on Ultrasound Diagnostic Criteria and New Ultrasound Severity and Activity Scorings of Hidradenitis Suppurativa: Modified SOS-HS and US-HSA. *J Ultrasound Med*. **2024**;43:207-213.
97. Mendes-Bastos, P.; Martorell, A.; Bettoli, V.; Matos, A.P.; Muscianisi, E.; Wortsman, X. The use of ultrasound and magnetic resonance imaging in the management of hidradenitis suppurativa: a narrative review. *Br J Dermatol*. **2023**;188:591-600.
98. Wortsman, X.; Reyes-Baraona, F.; Ramirez-Cornejo, C.; Ferreira-Wortsman, C.; Caposiena Caro, R.D.; Molina-Leyva, A.; Arias-Santiago, S.; Giavedoni, P.; Martorell, A.; Romani, J.; et al. Can Ultrasound

Preprints.org (www.preprints.org) | NOT PEER-REVIEWED | Posted: 24 December 2024 doi:10.20944/preprints202412.1938.v1

Examinations Generate Pain in Hidradenitis Suppurativa Patients? Results from a Multicentric Cross-Sectional Study. *Dermatology*. **2023**;239:277-282.

99. Iannone, M.; Janowska, A.; Oranges, T.; Balderi, L.; Benincasa, B.B.; Vitali, S.; Tonini, G.; Morganti, R.; Romanelli, M.; Dini, V. Ultrasound-guided injection of intralesional steroids in acute hidradenitis suppurativa lesions: A prospective study. *Dermatol Ther.* **2021**;34:e15068.
100. Sechi, A.; Patrizi, A.; Raone, B. Intralesional steroid injections to target sinus tract fibrosis in hidradenitis suppurativa: Results from an ultrasound-based retrospective study. *Dermatol Ther*. **2022**;35:e15710.
101. Dini, V.; Michelucci, A.; Granieri, G.; Zerbinati, N.; Margiotta, F.M.; Romanelli, M. Evaluation of post-surgical complications of hidradenitis suppurativa lesions explored with presurgical ultra-high frequency ultrasound mapping. *J Wound Care*. **2024**;33:S10-S16.
102. Michelucci, A.; Fidanzi, C.; Manzo Margiotta, F.; Granieri, G.; Salvia, G.; Janowska, A.; Romanelli, M.; Dini, V. Presurgical Mapping With Ultra-high Frequency Ultrasound of Hidradenitis Suppurativa Lesions Treated With Wide Local Excision and Secondary Intention Healing. *Dermatol Surg*. **2024**.
103. Wortsman, X.; Ortiz-Orellana, G.; Valderrama, Y.; Ferreira-Wortsman, C.; Reyes, F.; Herane, M.I. Ultrasonography of Facial and Submandibular Hidradenitis Suppurativa and Concomitance With Acne Vulgaris. *J Ultrasound Med*. **2024**;43:1919-1928.
104. Czarnecki, P.; Kopeć, J.; Przewratil, P. Sequential, ultrasound-guided, minimally invasive pit-picking procedure with Nd:YAG laser epilation treatment for pilonidal disease. *Pol Przegl Chir*. **2023**;96:13-16.
105. Kaiyasah. H.; Abufool, L.; Al Ozaibi, L. The Role of Point-of-Care Ultrasound in Pilonidal Sinus Disease. *POCUS J*. **2022**;7:205-207.
106. Yilmaz, T.U.; Yavuz, O.; Yirmibesoglu, A.O.; Sarisoy, H.T.; Vural, C.; Kiraz, U.; Utkan, N.Z. Radiological, Clinical, and Histological Findings in the Treatment of Pilonidal Sinus with Phenol Injection. *Medeni Med J*. **2022**;37:29-35.
107. Aksoy, H.M.; Aksoy, B.; Ozkur, E.; Calikoglu, E. Topical polyphenol treatment of sacrococcygeal pilonidal sinus disease: use of ultrasonography to evaluate response to treatment - clinical case series study. *Postepy Dermatol Alergol*. **2019**;36:431-443.
108. Puranik, C.I.; Wadhwani, V.J.; Vora, D.M. Role of transperineal ultrasound in infective and inflammatory disorders. *Indian J Radiol Imaging*. **2017**;27:482-487.
109. Berritto, D.; Iacobellis, F.; Rossi, C.; Reginelli, A.; Cappabianca, S.; Grassi, R. Ultra high-frequency ultrasound: New capabilities for nail anatomy exploration. *J Dermatol*. **2017**;44:43-46.
110. Szymoniak-Lipska, M.; Polańska, A.; Jenerowicz, D.; Lipski, A.; Żaba, R.; Adamski, Z.; Dańczak-Pazdrowska, A. High-Frequency Ultrasonography and Evaporimetry in Non-invasive Evaluation of the Nail Unit. *Front Med (Lausanne)*. **2021**;8:686470.
111. Ortner, V.K.; Mandel, V.D.; Bertugno, S.; Philipsen, P.A.; Haedersdal, M. Imaging of the nail unit in psoriatic patients:A sys-tematic scoping review of techniques and terminology. *Exp Dermatol*. **2022**;31:828-840.
112. Wortsman, X; Gutierrez, M; Saavedra, T.; Honeyman, J. The role of ultrasound in rheumatic skin and nail lesions: a mul-ti-specialist approach. *Clin Rheumatol*. **2011**;30:739-748.
113. Michelucci, A; Dini, V; Salvia, G; Granieri, G; Manzo Margiotta, F; Panduri, S; Morganti, R; Romanelli, M. Assessment and Monitoring of Nail Psoriasis with Ultra-High Frequency Ultrasound: Preliminary Results. *Diagnostics (Basel)*. **2023**;13:2716.
114. Krajewska-Włodarczyk, M; Owczarczyk-Saczonek, A. Usefulness of Ultrasound Examination in the Assessment of the Nail Apparatus in Psoriasis. *Int J Environ Res Public Health*. **2022**;19:5611.
115. Krajewska-Włodarczyk, M.; Żuber, Z; Owczarczyk-Saczonek, A. Ultrasound Evaluation of the Effectiveness of the Use of Acitretin in the Treatment of Nail Psoriasis. *J Clin Med*. **2021**;10:2122.
116. Sechi, A.; Wortsman, X.; Tosti, A.; Iorizzo, M. Advances in image-based diagnosis of nail disorders. *J Eur Acad Dermatol Venereol*. **2024** Sep 4. doi: 10.1111/jdv.20309. Epub ahead of print
117. Krajewska-Włodarczyk, M.; Owczarczyk-Saczonek, A.; Placek, W.; Wojtkiewicz, M.; Wiktorowicz, A.; Wojtkiewicz, J. Distal interphalangeal joint extensor tendon enthesopathy in patients with nail psoriasis. *Sci Rep*. **2019**;9:3628.

Preprints.org (www.preprints.org) | NOT PEER-REVIEWED | Posted: 24 December 2024 doi:10.20944/preprints202412.1938.v1

118. Michelucci, A.; Dini, V.; Salvia, G.; Granieri, G.; Manzo Margiotta, F.; Panduri, S.; Morganti, R.; Romanelli, M. Assessment and Monitoring of Nail Psoriasis with Ultra-High Frequency Ultrasound: Preliminary Results. *Diagnostics (Basel)*. **2023**;13:2716.
119. Aluja Jaramillo, F.; Quiasúa Mejía, D.C.; Martínez Ordúz, H.M.; González Ardila, C. Nail unit ultrasound: a complete guide of the nail diseases. *J Ultrasound*. **2017**;20:181-192.
120. Sechi, A.; Starace, M.; Piraccini, B.M.; Wortsman, X. Ultrasound Features of Onychopapilloma at High-Frequency and Ultra-High Frequency. *J Ultrasound Med*. **2024**;43:71-76.
121. Lee, D.K.; Lipner, S.R. Optimal diagnosis and management of common nail disorders. *Ann Med*. **2022**;54:694-712.
122. Turner, V.L.; Wortsman, X. Ultrasound Features of Nail Lichen Planus. *J Ultrasound Med*. **2024**;43:781-788.
123. Sechi, A.; Alessandrini, A.; Patrizi, A.; Starace, M.; Caposiena Caro, R.D.; Vara, G.; Brandi, N.; Golfieri, R.; Piraccini, B.M. Ultrasound features of the subungual glomus tumor and squamous cell carcinomas. *Skin Res Technol*. **2020**;26:867-875.
124. Silva, J.; Pinto, C.; Amorim-Alves, L. Digital Mucous Cyst: An Unusual Presentation of Osteoarthritis. *Acta Med Port*. **2022**;35:591-592.
125. Patel, R.A.; Ariza-Hutchinson, A.; Emil, N.S.; Muruganandam, M.; Nunez, S.E.; McElwee, M.K.; O'Sullivan, F.X.; Hayward, W.A.; Haseler, L.J.; Sibbitt, W.L. Jr. Intraarticular injection of the interphalangeal joint for therapy of digital mucoid cysts. *Rheumatol Int.* **2022**;42:861-868.
126. Sechi, A.; Starace, M.; Alessandrini, A.; Caposiena Caro, R.D.; Piraccini, B.M. Digital Myxoid Cysts: Correlation of Initial and Long-Term Response to Steroid Injections. *Dermatol Surg*. **2021**;47:e146-e152.
127. Vargas, E.A.T.; Finato, V.M.L.; Azulay-Abulafia, L.; Leverone, A.; Nakamura, R.; Wortsman, X. Ultrasound of Nails: Why, How, When. *Semin Ultrasound CT MR*. **2024**;45:233-250.
128. Crisan, D.; Wortsman, X.; Catalano, O.; Badea, R.; Kastler, S.; Badea, A.; Manea, A.; Scharffetter-Kochanek, K.; Strilciuc, S.; Crisan, M.; et al. Pre-operative high-frequency ultrasound: a reliable management tool in auricular and nasal non-melanoma skin cancer. *J Dtsch Dermatol Ges*. **2024**;22:357-365.
129. Russo, A.; Patanè, V.; Fusco, L.; Faggioni, L.; Boschetti, C.E.; Santagata, M.; Neri, E.; Cappabianca, S.: Reginelli, A. Reliability of Ultrasonographic Assessment of Depth of Invasion and Tumor Thickness in Intraoral Mucosa Lesions: A Preliminary Expe-rience. *J Clin Med*. **2024**;13:2595.
130. Simonetti, O.; Lucarini, G.; Rubini, C.; Lazzarini, R.; DI Primio, R.; Offidani, A. Clinical and prognostic significance of survivin, AKT and VEGF in primary mucosal oral melanoma. *Anticancer Res*. **2015**;35:2113-2120.
131. Del Puerto, C.; Wortsman, X.; Downey, C. Lingual Epidermal Choristoma: Ultrasonography as a Diagnostic Tool. *Dermatol Pract Concept*. **2024**;14:e2024014.
132. Buch, J.; Karagaiah, P.; Raviprakash, P.; Patil, A.; Kroumpouzos, G.; Kassir, M.; Goldust, M. Noninvasive diagnostic techniques of port wine stain. *J Cosmet Dermatol*. **2021**;20:2006-2014.
133. Rodríguez Bandera, A.I.; Feito Rodríguez, M.; Chiloeches Fernández, C.; Stewart, N.; Valdivielso-Ramos, M. Role of colour-Doppler high-frequency ultrasonography in capillary malformation-arteriovenous malformation syndrome: a case series. *Australas J Dermatol.* **2020**;61:349-352.
134. Chen, W.; Wang, Y.; Qi, H.; Wang, T. The diagnostic value of ultrasonography in evaluation of the intraneural vascular anomalies of peripheral nerves. *Acta Radiol*. **2024**;65:241-246.
135. Pragasam, S.; Kumari, R.; Munisamy, M.; Mohan Thappa, D. Utility of high-frequency ultrasound in assessing cutaneous edema in venous ulcer patients. *Skin Res Technol*. **2021**;27:904-908.
136. Liu, Q.; Zhou, J.; Wang, W.; Chen, X.; Xu, Y.; Huang, H.; Mi, J. A prospective study of super-thin anterolateral thigh flap harvesting assisted by high-frequency color Doppler ultrasound in detecting perforators in deep adipose layers. *Zhongguo Xiu Fu Chong Jian Wai Ke Za Zhi*. **2024**;38:62-68.
137. Hayashi ,A.; Giacalone, G.; Yamamoto, T.; Belva, F.; Visconti, G.; Hayashi, N.; Handa, M.; Yoshimatsu, H.; Salgarello, M. Ultra High-frequency Ultrasonographic Imaging with 70 MHz Scanner for Visualization of the Lymphatic Vessels. *Plast Reconstr Surg Glob Open*. **2019**;7:e2086.
138. Cowan, R.; Mann, G.; Salibian, A.A. Ultrasound in Microsurgery: Current Applications and New Frontiers. *J Clin Med*. **2024**;13:3412.

Preprints.org (www.preprints.org) | NOT PEER-REVIEWED | Posted: 24 December 2024 doi:10.20944/preprints202412.1938.v1

139. Visconti, G.; Hayashi, A.; Bianchi, A.; Tartaglione, G.; Bartoletti, R.; Salgarello, M. Lymphaticovenular Anastomosis for Advanced-Stage Peripheral Lymphedema: Expanding Indication and Introducing the Hand/Foot Sign. *J Plast Reconstr Aesthet Surg*. **2022**;75:2153-2163.
140. Pazdrowski, J.; Dańczak-Pazdrowska, A.; Polańska, A.; Kaźmierska, J.; Barczak, W.; Szewczyk, M.; Golusiński, P.; Adamski, Z.; Żaba, R.; Golusiński, W. An ultrasonographic monitoring of skin condition in patients receiving radiotherapy for head and neck cancers. *Skin Res Technol*. **2019**;25:857-861.
141. Garnier, M.; Champeaux, E.; Laurent, E.; Boehm, A.; Briard, O.; Wachter, T.; Vaillant, L.; Patat, F.; Bens, G.; Machet, L. High-frequency ultrasound quantification of acute radiation dermatitis: pilot study of patients undergoing radiotherapy for breast cancer. *Skin Res Technol*. **2017**;23:602-606.
142. Meikle, B.; Simons, M.; Mahoney, T.; Reddan, T.; Dai, B.; Kimble, R.M.; Tyack, Z. Ultrasound measurement of traumatic scar and skin thickness: a scoping review of evidence across the translational pipeline of research-to-practice. *BMJ Open*. **2024**;14:e078361.
143. Barrett, C.D.; Celestin, A.; Fish, E.; Glass, C.C.; Eskander, M.F.; Murillo, R.; Gospodinov, G.; Gupta, A.; Hauser, C.J. Surgical wound assessment by sonography in the prediction of surgical wound infections. *J Trauma Acute Care Surg*. **2016**;80:229-236.
144. Morroni, G.; Simonetti, O.; Brenciani, A.; Brescini, L.; Kamysz, W.; Kamysz, E.; Neubauer, D.; Caffarini, M.; Orciani, M.;, Giovanetti, E; et al. In vitro activity of Protegrin-1, alone and in combination with clinically useful antibiotics, against Acinetobacter baumannii strains isolated from surgical wounds. *Med Microbiol Immunol*. **2019**;208:877-883.
145. Tao, Y.; Wei, C.; Su, Y.; Hu, B.; Sun, D. Emerging High-Frequency Ultrasound Imaging in Medical Cosmetology. *Front Physiol*. **2022**;13:885922.
146. Krauze, A.; Woźniak, W.; Mlosek, R.K. Usefulness of high-frequency ultrasound to assess the healing progress of shin ulcers. *J Ultrason*. **2021**;20:e254-e260.
147. Tantray, M.D.; Rather, A.; Manaan, Q.; Andleeb, I.; Mohammad, M.; Gull, Y. Role of ultrasound in detection of radiolucent foreign bodies in extremities. *Strategies Trauma Limb Reconstr*. **2018**;13:81-85.
148. Viviano, S.L.; Chandler, L.K.; Keith, J.D. Ultrahigh Frequency Ultrasound Imaging of the Hand: A New Diagnostic Tool for Hand Surgery. *Hand (N Y)*. **2018**;13:720-725.
149. Crisan, D.; Tarnowietzki, E.; Bernhard, L.; Möller, M.; Scharffetter-Kochanek, K.; Crisan, M.; Schneider, L.A. Rationale for Using High-Frequency Ultrasound as a Routine Examination in Skin Cancer Surgery: A Practical Approach. *J Clin Med*. **2024**;13:2152.
150. Moscarella, E.; Brancaccio, G.; Briatico, G.; Ronchi, A.; Verolino, P.; Argenziano, G.; Alfano, R. Management of advanced basal cell carcinoma: Real-life data with sonidegib. *Dermatol Ther*. **2021**;34:e14948.
151. Laverde-Saad, A.; Simard, A.; Nassim, D.; Jfri, A.; Alajmi, A.; O'Brien, E.; Wortsman, X. Performance of Ultrasound for Identifying Morphological Characteristics and Thickness of Cutaneous Basal Cell Carcinoma: A Systematic Review. *Dermatology*. **2022**;238:692-710.
152. Catalano, O.; Crisan, D.; Díaz, C.P.G.; Cavallieri, F.; Varelli, C.; Wortsman, X. Ultrasound Assessment of Skin Tumors Local Recurrence. *J Ultrasound Med*. **2023**;42:2439-2446.
153. Basra, M.; Shapiro, L.; Patel, H.; Payne, C.; Brazen, B.; Biglione, A. Exploring the Utilization of Imaging Modalities in the Diagnosis of Basal Cell Carcinoma: A Scoping Review. *Cureus*. **2024**;16:e56047.
154. Bozsányi, S.; Boostani, M.; Farkas, K.; Hamilton-Meikle, P.; Varga, N.N.; Szabó, B.; Vasanits, F.; Kuroli, E.; Meznerics, F.A.; Lőrincz, K.; et al. Optically Guided High-Frequency Ultrasound to Differentiate High-Risk Basal Cell Carcinoma Subtypes: A Single-Centre Prospective Study. *J Clin Med*. **2023**;12:6910.
155. Russo, G.M.; Russo, A.; Urraro, F.; Cioce, F.; Gallo, L.; Belfiore, M.P.; Sangiovanni, A.; Napolitano, S.; Troiani, T.; Verolino, P.; et al. Management of Non-Melanoma Skin Cancer: Radiologists Challenging and Risk Assessment. *Diagnostics (Basel)*. **2023**;13:793.
156. Wortsman, X.; Vergara, P.; Castro, A.; Saavedra, D.; Bobadilla, F.; Sazunic, I.; Zemelman, V.; Wortsman, J. Ultrasound as predictor of histologic subtypes linked to recurrence in basal cell carcinoma of the skin. *J Eur Acad Dermatol Venereol*. **2015**;29:702-707.
157. Wortsman, X. Ultrasound in Skin Cancer: Why, How, and When to Use It? *Cancers (Basel)*. **2024**;16:3301.

Preprints.org (www.preprints.org) | NOT PEER-REVIEWED | Posted: 24 December 2024 doi:10.20944/preprints202412.1938.v1

158. Licata, G.; Scharf, C.; Ronchi, A.; Pellerone, S.; Argenziano, G.; Verolino, P.; Moscarella, E. Diagnosis and Management of Melanoma of the Scalp: A Review of the Literature. *Clin Cosmet Investig Dermatol*. **2021**;14:1435-1447.
159. Varga, N.N.; Boostani, M.; Farkas, K.; Bánvölgyi, A.; Lőrincz, K.; Posta, M.; Lihacova, I.; Lihachev, A.; Medvecz, M.; Holló, P.; et al. Optically Guided High-Frequency Ultrasound Shows Superior Efficacy for Preoperative Estimation of Breslow Thickness in Comparison with Multispectral Imaging: A Single-Center Prospective Validation Study. *Cancers (Basel)*. **2023**;16:157.
160. Reginelli, A.; Russo, A.; Berritto, D.; Patane, V.; Cantisani, C.; Grassi, R. Ultra-High-Frequency Ultrasound: A Modern Diagnostic Technique for Studying Melanoma. *Ultraschall Med*. **2023**;44:360-378. English, German.
161. Belfiore, M.P.; Reginelli, A.; Russo, A.; Russo, G.M.; Rocco, M.P.; Moscarella, E.; Ferrante, M.; Sica, A.; Grassi, R.; Cappabianca, S. Usefulness of High-Frequency Ultrasonography in the Diagnosis of Melanoma: Mini Review. *Front Oncol*. **2021**;11:673026.
162. Reginelli, A.; Belfiore, M.P.; Russo, A.; Turriziani, F.; Moscarella, E.; Troiani, T.; Brancaccio, G.; Ronchi, A.; Giunta, E.; Sica, A:, et al. A Preliminary Study for Quantitative Assessment with HFUS (High- Frequency Ultrasound) of Nodular Skin Melanoma Breslow Thickness in Adults Before Surgery: Interdisciplinary Team Experience. *Curr Radiopharm*. **2020**;13:48-55.
163. Płocka, M.; Czajkowski, R. High-frequency ultrasound in the diagnosis and treatment of skin neoplasms. *Postepy Dermatol Alergol*. **2023**;40:204-207.
164. Hernández-Aragüés, I.; Vázquez-Osorio, I.; Alfageme, F.; Ciudad-Blanco, C.; Casas-Férnandez, L.; Rodríguez-Blanco, M.I.; Suárez-Fernández, R. Skin ultrasound features of Merkel cell carcinoma. *J Eur Acad Dermatol Venereol*. **2017**;31:e315-e318.
165. Sica, A.; Vitiello, P.; Caccavale, S.; Sagnelli, C.; Calogero, A.; Doraro, C.A.; Pastore, F.; Ciardiello, F.; Argenziano, G.; Reginelli, A.; et al. Primary Cutaneous DLBCL Non-GCB Type: Challenges of a Rare Case. *Open Med (Wars)*. **2020**;15:119-125.
166. Russo, A.; Patanè, V.; Gagliardi, F.; Urraro, F.; Ronchi, A.; Vitiello, P.; Sica, A.; Argenziano, G.; Nardone, V.; Reginelli, A. Preliminary Experience in Ultra-High Frequency Ultrasound Assessment of Cutaneous Primary Lymphomas: An Innovative Classification. *Cancers (Basel)*. **2024** ;16:2456.
167. Wohlmuth-Wieser, I.; Ramjist, J.M.; Shear, N.; Alhusayen, R. Morphologic Features of Cutaneous T-Cell Lymphomas Using Dermoscopy and High Frequency Ultrasound. J Clin Med. 2020;10:17
168. Wang, J.; Liu, J. Dermoscopy and high-frequency ultrasound provide diagnostic clues in a gastric adenocarcinoma with cutaneous metastasis as the initial presentation: A case report. *Skin Res Technol*. **2023**;29:e13380.
169. Solivetti, F.M.; Elia, F.; Latini, A.; Cota, C.; Cordiali-Fei, P.; Di Carlo, A. AIDS-Kaposi Sarcoma and Classic Kaposi Sarcoma: are different ultrasound patterns related to different variants? *J Exp Clin Cancer Res*. **2011**;30:40
170. Li, L.; Xu, J.; Wang, S.; Yang, J. Ultra-High-Frequency Ultrasound in the Evaluation of Paediatric Pilomatricoma Based on the Histopathologic Classification. *Front Med (Lausanne)*. **2021**;8:673861.
171. Rodríguez Bandera, A.I.; Moreno Bonilla, G.; Feito Rodríguez, M.; Beato Merino, M.J.; de Lucas Laguna, R. Jellyfish-like sonographic pattern can help recognition of dermatofibrosarcoma protuberans. Report of 3 new cases and review of the literature. *Australas J Dermatol*. **2019**;60:e148-e150.
172. Zou, M.H.; Huang, Q.; Yang, T.; Jiang, Y.; Zhang, L.J.; Xie, Y.; Zheng, R.Q. Role of ultrasound in the diagnosis of primary and recurrent dermatofibrosarcoma protuberans. *BMC Cancer*. **2021**;21:909.
173. Crisan, D.; Schneider, L.A.; Scharffetter-Kochanek, K.; Bernhard, L.; Crisan, M.; Wortsman, X. The Usefulness of Ultrasonography for Supporting the Differentiation, Diagnosis, and Treatment of Atypical Fibroxanthoma and Pleomorphic Dermal Sarcoma. *J Ultrasound Med*. **2024**;43:1563-1572.
174. Helbig, D.; Ziemer, M.; Dippel, E.; Erdmann, M.; Hillen, U.; Leiter, U.; Mentzel, T.; Osterhoff, G.; Ugurel, S.; Utikal, J.; et al. S1-guideline atypical fibroxanthoma (AFX) and pleomorphic dermal sarcoma (PDS). *J Dtsch Dermatol Ges*. **2022**;20:235-243.

Preprints.org (www.preprints.org) | NOT PEER-REVIEWED | Posted: 24 December 2024 doi:10.20944/preprints202412.1938.v1

175. Carletti, M.; Nguyen, D.A.; Malouf, P.; Ingersoll, Z.; Hosler, G.A.; Weis, S.E. Pleomorphic Dermal Sarcoma: A Clinical and Histopathologic Emulator of Atypical Fibroxanthoma, but Different Biologic Behavior. *HCA Healthc J Med*. **2022**;3:299-304.
176. Taleb, E.; Saldías, C.; Gonzalez, S.; Misad, C.; Wortsman, X. Sonographic Characteristics of Leiomyomatous Tumors of Skin and Nail: a Case Series. *Dermatol Pract Concept*. **2022**;12:e2022082.
177. Hobayan, C.G.P.; Gray, A.N.; Waters, M.F.; Mager, L.A.; Kobayashi, S.; Essien, E.W.; Ulman, C.A.; Kaffenberger, B.H. Diagnostic accuracy of high-frequency ultrasound for cutaneous neoplasms: a narrative review of the literature. *Arch Dermatol Res*. **2024**;316:419
178. Li, D.; Yang, F.; Zhao, Y.; Wang, Q.; Ren, W.; Sun, L.; Shan, D.; Qin, C. High-Frequency Ultrasound Imaging to Distinguish High-Risk and Low-Risk Dermatofibromas. *Diagnostics (Basel)*. **2023**;13:3305.
179. Mlosek, R.K.; Malinowska, S.P. High-Frequency Ultrasound in the Assessment of Cellulite-Correlation between Ultrasound-Derived Measurements, Clinical Assessment, and Nürnberger-Müller Scale Scores. *Diagnostics (Basel)*. **2024**;14:1878.
180. Mlosek, R.K.; Dębowska, R.M.; Lewandowski, M.; Malinowska, S.; Nowicki, A.; Eris, I. Imaging of the skin and subcutaneous tissue using classical and high-frequency ultrasonographies in anti-cellulite therapy. *Skin Res Technol*. **2011**;17:461-8.
181. Mlosek, R.K.; Woźniak, W.; Malinowska, S.; Lewandowski, M.; Nowicki, A. The effectiveness of anticellulite treatment using tripolar radiofrequency monitored by classic and high-frequency ultrasound. *J Eur Acad Dermatol Venereol*. **2012**;26:696-703.
182. Whipple, L.A.; Fournier, C.T.; Heiman, A.J.; Awad, A.A.; Roth, M.Z.; Cotofana, S.; Ricci, J.A. The Anatomical Basis of Cellulite Dimple Formation: An Ultrasound-Based Examination. *Plast Reconstr Surg*. **2021**;148:375e-381e.
183. Sandby-Møller, J.; Wulf, H.C. Ultrasonographic subepidermal low-echogenic band, dependence of age and body site. *Skin Res Technol.* **2004**;10:57-63. doi:..
184. Crisan, D.; Roman, I.; Crisan, M.; Scharffetter-Kochanek, K.; Badea, R. The role of vitamin C in pushing back the boundaries of skin aging: an ultrasonographic approach. *Clin Cosmet Investig Dermatol*. **2015**;8:463-470.
185. Pequeno, A.L.V.; Bagatin, E. Dermatological ultrasound in assessing skin aging. *Front Med (Lausanne)*. **2024**;11:1353605.
186. Czajkowska, J.; Juszczyk, J.; Bugdol, M.N.; Glenc-Ambroży, M.; Polak, A.; Piejko, L.; Pietka, E. High-frequency ultrasound in anti-aging skin therapy monitoring. *Sci Rep*. **2023**;13:17799.
187. Salvia, G.; Zerbinati, N.; Manzo Margiotta, F.; Michelucci, A.; Granieri, G.; Fidanzi, C.; Morganti, R.; Romanelli, M.; Dini, V. Ultra-High-Frequency Ultrasound as an Innovative Imaging Evaluation of Hyaluronic Acid Filler in Nasolabial Folds. *Diagnostics (Basel).* **2023**;13:2761.
188. Cavallieri, F.A.; Balassiano, L.K.A.; Munhoz, G.; Tembra, M.F.; Wortsman, X. Ultrasound in Aesthetics: Filler and Non-Filler Applications. *Semin Ultrasound CT MR*. **2024**;45:251-263.
189. Wortsman, X. Identification and Complications of Cosmetic Fillers: Sonography First. *J Ultrasound Med*. **2015**;34:1163-1172.
190. Wortsman, X.; Quezada, N.; Peñaloza, O.; Cavallieri, F.; Schelke, L.; Velthuis, P. Ultrasonographic Patterns of Calcium Hydroxyapatite According to Dilution and Mix With Hyaluronic Acid. *J Ultrasound Med*. **2023**;42:2065-2072.
191. Wortsman, X.; Quezada, N. Ultrasound Morphology of Polycaprolactone Filler. *J Ultrasound Med*. **2017**;36:2611-2615.
192. Wortsman X. Top applications of dermatologic ultrasonography that can modify management. Ultrasonography. 2023;42:183-202.
193. Sigrist, R.; Fassina, M.; Wortsman, X. Ultrasonographic Pattern of a New Generation of Polymethylmethacrylate at High-Frequency and Ultra-High Frequency. *Dermatol Surg*. **2024**. doi: 10.1097/DSS.0000000000004422. Epub ahead of print
194. Sigrist, R.; Noronha, G.; Quezada, N.; Wortsman, X. Ultrasonographic Pattern of Poly- l -Lactic Acid at High-Frequency and Ultrahigh-Frequency. *Dermatol Surg*. **2024**;50:783-785.

Preprints.org (www.preprints.org) | NOT PEER-REVIEWED | Posted: 24 December 2024 doi:10.20944/preprints202412.1938.v1

195. Bravo, B.S.F.; de Almeida, T.S.C.; Carvalho, R.M.; Machado, C.J.; Bravo, L.G.; Elias, M.C. Dermal Thickness Increase and Aesthetic Improvement with Hybrid Product Combining Hyaluronic Acid and Calcium Hydroxyapatite: A Clinical and Sonographic Analysis. *Plast Reconstr Surg Glob Open*. **2023**;11:e5055.
196. Casabona, G.; Kaye, K.; Cotofana, S.; Davidovic, K.; Alfertshofer, M.; Freytag, L. Histological effects of a combined collagen stimulation procedure consisting of microfocused ultrasound, soft tissue filler, and Ca-HA injections. *J Cosmet Dermatol*. **2023**;22:1724-1730.
197. Qiao, J.; Jia, Q.N.; Jin, H.Z.; Li, F.; He, C.X.; Yang, J.; Zuo, Y.G.; Fu, L.Q. Long-Term Follow-Up of Longevity and Diffusion Pattern of Hyaluronic Acid in Nasolabial Fold Correction through High-Frequency Ultrasound. *Plast Reconstr Surg*. **2019**;144:189e-196e.
198. Turlier, V.; Rouquier, A.; Black, D.; Josse, G.; Auvergnat, A.; Briant, A.; Dahan, S.; Gassia, V.; Saint-Martory, C.; Zakaria, W.; et al. Assessment of the clinical efficacy of a hyaluronic acid-based deep wrinkle filler using new instrumental methods. *J Cosmet Laser Ther*. **2010**;12:195-202.
199. Urdiales-Gálvez, F.; Delgado, N.E.; Figueiredo, V.; Lajo-Plaza, J.V.; Mira, M.; Ortíz-Martí, F.; Del Rio-Reyes, R.; Romero-Álvarez, N.; Del Cueto, S.R.; Segurado, M.A.; Rebenaque, C.V. Preventing the Complications Associated with the Use of Dermal Fillers in Facial Aesthetic Procedures: An Expert Group Consensus Report. *Aesthetic Plast Surg*. **2017**;41:667-677.
200. Jiang, L.; Yuan, L.; Li, Z.; Su, X.; Hu, J.; Chai, H. High-Frequency Ultrasound of Facial Filler Materials in the Nasolabial Groove. *Aesthetic Plast Surg*. **2022**;46:2972-2978.
201. Chai, H.; Su, X.; Yuan, L.; Li, Z.; Jiang, L.; Liu, Y.; Dou, M.; Hu, J. High-Frequency Ultrasound Imaging Findings of Different Mental Injectable Soft Tissue Fillers. *Aesthetic Plast Surg*. **2022**;46:2995-3002
202. Jiang, L.; Yuan, L.; Su, X.; Zhen, Q.; Jia, Y.; Hu, J.; Chai, H. The Application of High-frequency Ultrasonic Imaging in Identifying Fillers in the Temporal Region. *Plast Reconstr Surg Glob Open*. **2023**;11:e5269.
203. Sigrist, R.; Desyatnikova, S.; Chammas, M.C.; Vasconcelos-Berg, R. Best Practices for the Use of High-Frequency Ultrasound to Guide Aesthetic Filler Injections-Part 1: Upper Third of the Face. *Diagnostics (Basel)*. **2024**;14:1718.
204. Weiner, S.F. Ultrasound for the Aesthetic Injector. *Plast Aesthet Nurs (Phila)*. **2022**;42:88-98.
205. Velthuis, P.J.; Jansen, O.; Schelke, L.W.; Moon, H.J.; Kadouch, J.; Ascher, B.; Cotofana, S. A Guide to Doppler Ultrasound Analysis of the Face in Cosmetic Medicine. Part 1: Standard Positions. *Aesthet Surg J*. **2021**;41:NP1621-NP1632
206. Vasconcelos-Berg, R.; Izidoro, J.F.; Wenz, F.; Müller, A.; Navarini, A.A.; Sigrist, R.M.S. Doppler Ultrasound-Guided Filler Injections: Useful Tips to Integrate Ultrasound in Daily Practice. *Aesthet Surg J*. **2023**;43:773-783.
207. Desyatnikova, S.; Sigrist, R.; Wortsman, X. Forehead Ultrasound Anatomy: The Current Debate and a Way to Consensus. *Aesthet Surg J*. **2024**:sjae186.
208. Desyatnikova, S. Ultrasound-Guided Temple Filler Injection. *Facial Plast Surg Aesthet Med*. **2022**;24:501-503.
209. Desyatnikova, S.; Barrera, P. High-Resolution Ultrasound for Diagnosis and Treatment of Filler-Related Septal Necrosis. *Plast Reconstr Surg Glob Open*. **2024**;12:e5630.
210. Desyatnikova, S.; Mangieri, L. Nitrous Oxide Improves Tissue Perfusion in Vascular Occlusion Management. *Plast Reconstr Surg Glob Open*. **2023**;11:e5154.
211. Schelke, L.; Lowrey, N.; Mojallal, A.; Rowland-Warmann, M.J.; Wortsman, X.; Sigrist, R.M.; Velthuis, P.J.; Cotofana, S. Post-Treatment Displacement of Facial Soft Tissue Fillers-A Retrospective Ultrasound-based Investigation of 382 Zygomatic Regions. *Dermatol Surg*. **2024**;50:946-952.
212. Kroumpouzos, G.; Harris, S.; Bhargava, S.; Wortsman, X. Complications of fillers in the lips and perioral area: Prevention, assessment, and management focusing on ultrasound guidance. *J Plast Reconstr Aesthet Surg*. **2023**;84:656-669.
213. Mlosek, R.K.; Skrzypek, E.; Skrzypek, D.M.; Malinowska, S. High-frequency ultrasound-based differentiation between nodular dermal filler deposits and foreign body granulomas. *Skin Res Technol*. **2018**;24:417-422.
214. Mlosek, R.K.; Migda, B.; Skrzypek, E.; Słoboda, K.; Migda, M. The use of high-frequency ultrasonography for the diagnosis of palpable nodules after the administration of dermal fillers. *J Ultrason*. **2021**;20:e248-e253.

Preprints.org (www.preprints.org) | NOT PEER-REVIEWED | Posted: 24 December 2024 doi:10.20944/preprints202412.1938.v1

215. Cerón Bohórquez, J.M.; Desyatnikova, S. Ultrasound-guided Treatment of Polycaprolactone Granuloma. *Plast Reconstr Surg Glob Open*. **2024**;12:e5610.
216. Gatica, J.L.; Ortega, R.; Aragón-Caqueo, D.; Wortsman, X.; Sazunic, I.; Loubies, R. Granulomatous Reaction Secondary to Fractional Radiofrequency Microneedling with Clinical, Ultrasonographic, and Histologic Correlation. *Facial Plast Surg Aesthet Med*. **2024**;26:529-531.
217. Gonzalez, C.; Rengifo, J.; Macias-Arias, P.; Duque-Clavijo, V.; Noreña-Rengifo, B.D. High-Resolution Ultrasound for Complications of Botulinum Toxin Use: A Case Series and Literature Review. *Cureus*. **2024**;16:e63232.
218. Del Vecchio, D.; Kenkel, J.M. Practice Advisory on Gluteal Fat Grafting. *Aesthet Surg J*. **2022**;42:1019-1029.
219. Tillo, O.; Nassab, R.; Pacifico, M.D. The British Association of Aesthetic Plastic Surgeons (BAAPS) Gluteal Fat Grafting Safety Review and Recommendations. *Aesthet Surg J*. **2023**;43:675-682.
220. Vidal-Laureano, N.; Huerta, C.T.; Perez, E.A.; Earle, S.A. Augmented Safety Profile of Ultrasound-Guided Gluteal Fat Transfer: Retrospective Study With 1815 Patients. *Aesthet Surg J*. **2024**;44:NP263-NP270.
221. Elsaftawy, A.; Ostrowski, P.; Bonczar, M.; Stolarski, M.; Gabryszuk, K.; Bonczar, T. Buttock Augmentation with Ultrasonic Liposuction and Ultrasound-Guided Fat Grafting: A Retrospective Analysis Based on 185 Patients. *J Clin Med*. **2024**;13:1526.
222. Elsaftawy, A.; Ostrowski, P.; Bonczar, M.; Stolarski, M.; Gabryszuk, K.; Bonczar, T. Enhancing Buttock Contours: A Safer Approach to Gluteal Augmentation with Ultrasonic Liposuction, Submuscular Implants, and Ultrasound-Guided Fat Grafting. *J Clin Med*. **2024**;13:2856.
223. Wang, B.; He, P.; Zhao, R. B-ultrasound-assisted gluteal fat grafting in Asians: A prospective study of quantitative results from three-dimensional imaging and B-ultrasound analysis. *J Plast Reconstr Aesthet Surg*. **2024**;94:12-19.
224. Durán Vega, H.C.; Manzaneda, R.; Flores, E.; Manfrim, C.; Morelli, H. Deep Back Liposuction: Ultrasound-Guided Deep Fat Liposuction of the Subiliac Crest. *Aesthet Surg J*. **2024**;44:296-301.
225. Wortsman, X. Key Points to Select a Device for Dermatologic Ultrasound. *J Ultrasound Med*. **2023**;42:1367-1369.
226. Wortsman, X. Top Advances in Dermatologic Ultrasound. *J Ultrasound Med*. **2023**;42:521-545.
227. Gagliardi, F.; Russo, A.; Scharf, C.; Pinto, A.; Faenza, M.; D'Ippolito, E.; Argenziano, G.; Troiani, T.; Reginelli, A.; Nardone, V. All for one: Collaboration between dermatologist, radiation oncologist and radiologist in the clinical management of "difficult to treat" non melanoma skin cancer. *Clin Transl Radiat Oncol*. **2024**;46:100774.
228. Garcia, C.; Wortsman, X.; Bazaes-Nuñez, D.; Pelizzari, M.; Gonzalez, S.; Cossio, M.L.; De Barbieri, F. Skin sonography in children: a review. *Pediatr Radiol*. **2022**;52:1687-1705.
229. Sechi, A.; Patrizi, A.; Vincenzi, C.; Savoia, F.; Tartari, F.; Leuzzi, M.; Di Altobrando, A.; Besagni, F.; Merli, Y.; Neri, I. Sonographic features of vaccination granulomas in children with delayed-type hypersensitivity to aluminum. *Pediatr Dermatol*. **2019**;36:1012-1016.
230. Sechi, A.; Patrizi, A.; Vara, G.; Golfieri, R.; Neri, I. Keep CALME (childhood asymmetry labium majus enlargement) and follow up. *J Dtsch Dermatol Ges*. **2021**;19:1276-1281.
231. Gonzalez, C.; Wortsman, X. How to Start on Dermatologic Ultrasound: Basic Anatomical Concepts, Guidelines, Technical Considerations, and Best Tips. *Semin Ultrasound CT MR*. **2024**;45:180-191.
232. Perez-Sanchez, A.; Bambekova, P.G.; Owen, J.L.; Mader, M.; Wortsman, X.; Soni, N.J. Barriers to dermatologic ultrasound: A national survey of dermatologists in the US Veterans Affairs health care system. *JAAD Int*. **2022**;9:108-109.
233. Hoppmann, R.A.; Mladenovic, J.; Melniker, L.; Badea, R.; Blaivas, M.; Montorfano, M.; Abuhamad, A.; Noble, V.; Hussain, A.; Prosen, G.; et al. International consensus conference recommendations on ultrasound education for undergraduate medical students. Ultrasound J. **2022**;14:31.
234. Tagliati, C.; Rizzetto, G.; Molinelli, E.; De Simoni, E.; Fogante, M.; Argalia, G.; Lanni, G.; Rebonato, A.; Burroni, L.; Giuseppetti G.M.; et al. Does dermatoradiology exist? *Acta Dermatovenerol Alp Pannonica Adriat*. **2024**;33:107-108.
235. Wortsman, X. A New Imaging Subspecialty, Dermatologic Ultrasound: Letter from the Guest Editor. *Semin Ultrasound CT MR*. **2024**;45:179.

Preprints.org (www.preprints.org) | NOT PEER-REVIEWED | Posted: 24 December 2024 doi:10.20944/preprints202412.1938.v1

236. Cao, L.L.; Yang, Z.G.; Qi, W.H.; Zhang, H.; Bi, Y.; Shan, Y.; Cui, X.W.; Jiang, F. A preliminary study on ultrasound techniques applied to evaluate the curative effect of botulinum toxin type a in hypertrophic scars. *Heliyon*. **2024**;10:e34723.

Disclaimer/Publisher's Note: The statements, opinions and data contained in all publications are solely those of the individual author(s) and contributor(s) and not of MDPI and/or the editor(s). MDPI and/or the editor(s) disclaim responsibility for any injury to people or property resulting from any ideas, methods, instructions or products referred to in the content.